DEPARTMENT OF OCEAN ENGINEERING

MASSACHUSETTS INSTITUTE OF TECHNOLOGY

CAMBRIDGE, MASSACHUSETTS 02139

Vibration Problems of Rotating Machinery
Due to Coupling Misalignments

Frederick Lee Barber III

Course 13 A

May 1988

VIBRATION PROBLEMS OF ROTATING MACHINERY DUE TO COUPLING MISALIGNMENTS

by

FREDERICK LEE BARBER

B.S. Elect. Eng., University of Kansas
(1979)

Submitted to the Department of
OCEAN ENGINEERING
in Partial Fulfillment of the
Requirements for the Degrees of

NAVAL ENGINEER

and

MASTER OF SCIENCE IN MECHANICAL ENGINEERING

at the

MASSACHUSETTS INSTITUTE OF TECHNOLOGY

May 1988

ABSTRACT

Vibrational analysis of rotating machinery is able to identify a large number of system ills. Shaft bow, shaft unbalance and coupling misalignments make up the major portion of the observed vibrational frequency spectra of rotating machinery. These vibrational spectra can be used to determine the type of rotating system abnormality, the degree of misalignment and the rate of alignment degradation.

The proper joining of rotating machinery is a critical issue with high power and high speed equipments. Couplings used to join machinery have a broad spectrum of characteristics and specific purposes. Couplings are used to compensate for axial, lateral and angular misalignments. In addition, couplings may exhibit constant or non-constant input versus output speed relationships. The importance of mating a driving and driven piece of equipment with the properly designed coupling is paramount.

In the following report the author discusses numerous types of couplings, the behavioral characteristics of couplings and the considerations which must be taken into account when selecting a coupling for a rotating system. The analysis which follows lists the various alignment discrepancies which can be detected by vibrational analysis and the requirements for non-constant and constant velocity characteristics of couplings. In addition, numerous types of couplings are catalogued and discussed.

TABLE OF CONTENTS

LIST OF ILLUSTRATIONS

LIST OF ILLUSTRATIONS (continued)

LIST OF TABLES

1.0 INTRODUCTION

Misalignment is an important cause of vibration problems in rotating machinery. Misalignment in the context of this thesis includes any deviation from the ideal case in which a straight shaft rotates in perfectly aligned bearings. Misalignment can apply to a single piece of rotating equipment with a bent shaft or a straight shaft forced to rotate in three or more bearings which are not coaxially aligned. It can apply to two or more pieces of coupled machinery whose shafts are not properly aligned. In this thesis a survey is made of the various types of misalignments often encountered in rotating machinery and the vibrational characteristics which arise due to these misalignments are examined. In particular lateral, axial and angular coupling misalignments will be studied as a function of flexible coupling vibrational behavior. This discussion will include bent or bowed rotors, close-coupled systems, constant and non-constant velocity flexible couplings and axial motion couplings.

The coupling of driving to driven pieces of rotating machinery has historically been a problem in turbo-machinery

engineering. Once the idea of segregating the driven and driving mechanisms onto separate shafts developed, coupling issues have arisen. Numerous techniques for joining these shafts have evolved. These methods can briefly be generalized into three catagories: 1) close-coupled shafts which includes all mechanisms which directly fasten (usually bolted) axially aligned driving to driven shafts; 2) belt, chain or gear driven couplings in which parallel but radially offset shafts are joined, quite often through speed increasing or decreasing wheel ratios; 3) flexible coupled shafts engulf all fastening mechanisms in which a coupling is inserted between the driving and driven shaft for purposes of easing the joining procedure. The later category of couplings can accommodate misalignments (either intentional or unintentional) in angular, lateral and/or axial directions.

This paper will focus on how a coupling malady can be detected through vibrational analysis. The trend to build larger and higher speed drive mechanisms has increased incidences of coupling problems. In addition to the higher speed and horsepower requirements, the operating environment places a premium on quietness and minimal mechanical vibration to reduce personnel and equipment degradation. Quietly operating machinery operating in a work place will improve worker productivity. In Naval applications quietly

operating machinery translates into reduced detectability. Most coupling abnormalities cause vibrational problems which are easily detected by current state-of-the-art spectrum analyzers and shaft orbit detectors. Current coupling wisdom states that coupling problems tend to show up as vibrations with frequencies corresponding to 1/2, 1 or 2 times the operating angular velocity (Maxwell, 1980). A frequency spectrum similar to figure 1-1 may result from a poorly coupled rotating system. A perfectly aligned coupling would exhibit none of these spikes where as a vibrational problem may be characterized by a single spike or combination of spikes. The following pages will discuss causes for each of these spikes independently and then show how through superposition principles, a number of misalignment conditions can yield spectra similar to figure 1-1. It should be noted here that directionality of the above spectra has not been specified but rather lumped. Vibrations could be either axial, radial or torsional in direction. A specific coupling problem could yield vibrations in one or all of the above directions. In the specific discussions which follow directionality will be specified. The organization which follows will take the shaft coupling problem through an evolving chronology from simple to complex geometric shaft arrangements.

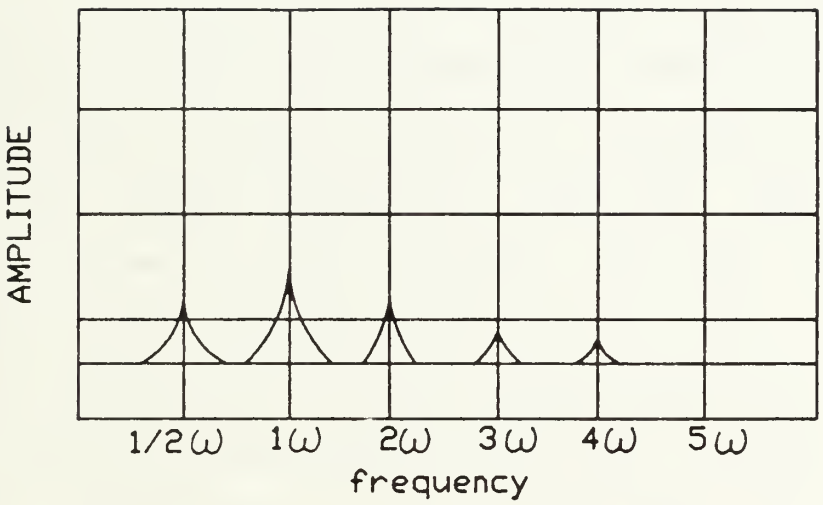

Generic frequency spectra for rotating machinery.

FIGURE 1-1

2.0 SINGLE SHAFT VIBRATIONS

A single uncoupled rotor may exhibit vibration problems for a variety of reasons. Sources of these vibrations may include shaft bearing misalignments, bowed rotors and mass unbalance. Bearing-shaft misalignments may from the vibrational analysis point of view be the hardest to detect. A shaft-bearing misalignment occurs when the bearing journal placements are not axially concentric and a straight shaft is forcefully fitted into the bearings. Figure 2-1 depicts an extreme case of a shaft distorted by bearings not axially aligned. The forces exerted by each of the bearing foundations cause the shaft to bend. As this forcefully bent shaft rotates, the forces exerted by the foundations remain constant as the shaft rotates at its operating angular velocity. Consequently, vibrational energy is not cyclically transmitted to the foundations or to the receivers at the sensing transducer (accelerometers) sites. Although not readily detectable with accelerometer and spectrum analyzer techniques, the misaligned bearing case is worth examining in some detail prior to proceeding on to other cases.

When the shaft in a misaligned journal set rotates one

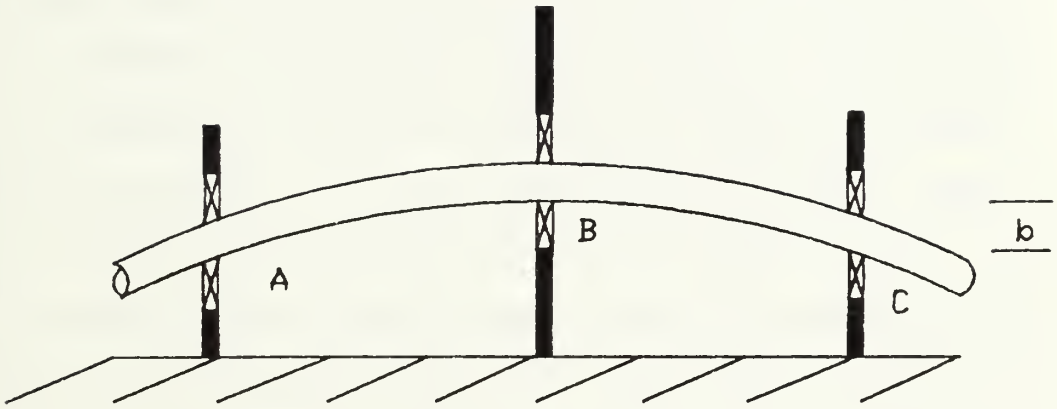

Shaft placed in misaligned bearings.

FIGURE 2-1

revolution, the shaft bends with the displacement of the shaft at point B being equal to the offset "b" of figure 2-1. This is similar to an ordinary beam in bending except that the bending action is angularly continuous throughout the rotation of the shaft. Consequently, as the shaft rotates through say one revolution the shaft outer fibers go through a tension-compression cycle. These alternating tension to compression cycles give rise to lateral fatigue loadings on the shaft. In the case of a simple beam, laterally loaded fatigue fracture can take place after a specific number of cycles providing the applied stresses are above the fatigue endurance limit of the shaft material. Fracture mechanics theory holds and the lower the applied stress the greater the number of cycles which can be withstood prior to fracture. In general, fatigue loading can be broken down into two categories. In low-cycle fatigue, fracture after 10^3 cycles is usually considered where as in "high-cycle fatigue" fracture after several million cycles is considered (Masabuchi, 1980). For a motor driven shaft operating at 1800 revolutions per minute cyclic loading of the misaligned shaft occurs at a rate equal to 30 cycles per second. Table 2-1 shows the load cycles for various periods of time. As can be readily seen for continuously operated machinery we are concerned with "high-cycle" fatigue loading. Fatigue fracture takes place primarily in three stages: 1) crack initiation, 2) crack

TIME	CYCLES
1 hour	$108X10^{3}$
1 day	$2.6X10^{6}$
1 week	$18.1X10^{6}$
1 month	$77X10^{6}$
1 year	$933X10^{6}$

Cyclic loading rates for a misaligned shaft operating at 1800 rpm.

TABLE 2-1

slow growth and 3) unstable fracture. Fatigue crack initiation is generally started at the surface at some site of manufacture or fabrication imperfection. Hence, highly polished surfaces will resist crack initiation. Once a crack is initiated crack growth is slow but continuous as the cyclic loading is continued. As the crack propagates laterally through the shaft the residual stress on the shaft cross section increases since the effective cross sectional area of the shaft is decreasing. Similar to repeated bending of a piece of stiff wire, as the number of bending cycles is increased the resistance to bending becomes less. As the crack propagates with each cycle, the crack growth rate also increases with each loading cycle. This crack growth continues until the remaining effective shaft cross section is unable to support the load onset by the misaligned bearings and the shaft fractures causing a catastrophic failure.

2.1 ROTATING MACHINERY ON A MOVING PLATFORM

A great deal of effort is extended to ensure rotating machinery shafts and bearings are axially aligned. However, with machinery placed on moving platforms such as ships, aircraft or automobiles this alignment may be distorted due to motion of the vehicle. For example a Naval ship may have drive shafts extending for 150 feet or more from a main engine to a propeller. The ship when at sea may experience bending motions brought on by various sea states and loading conditions. In these cases, as the ship moves across the waves a repeated bending of the shaft may occur (See figure 2-2). As the ship moves through the waves, the ship and thus the shafting is subjected to repeated bending in the lateral direction. In propulsion equipment the rotating angular velocity of the machinery is usually much faster than the lateral loading cycles. This in essence makes the case of the ship much the same as the misaligned journal bearing case just discussed. Once again looking at high cycle fatigue, we are concerned with fracture after several million loading cycles. For a ship operating at 200 shaft revolutions per minute table 2-2 indicates the time required to accumulate relatively large numbers of cycles. Therefore ensuring shaft bearing alignment may not always be sufficient. In cases of machinery mounted on mobile

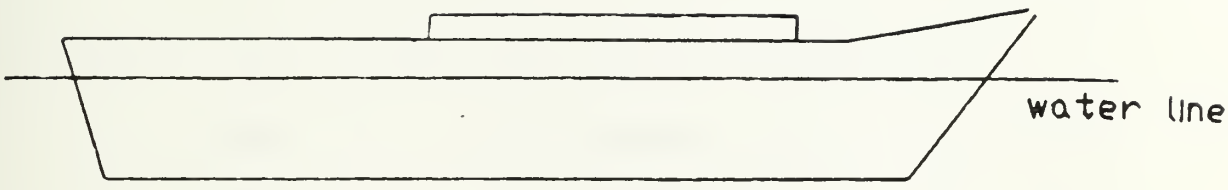

(a) vessel in calm water

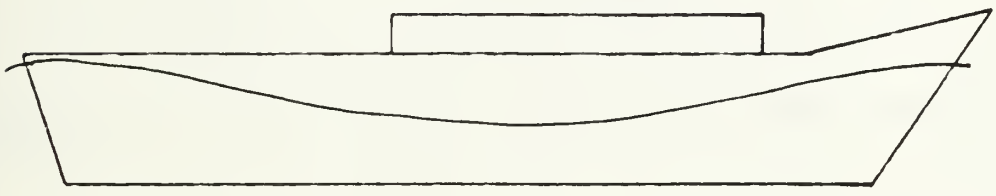

(b) vessel in sagging condition

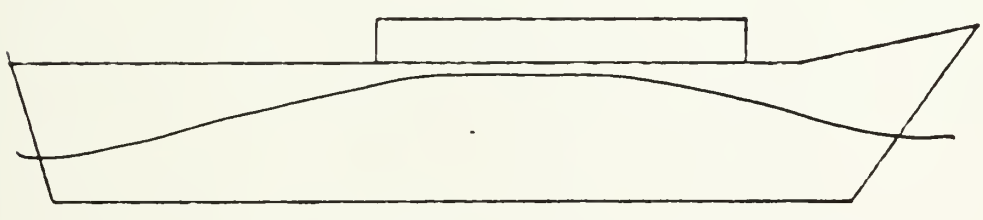

(c) vessel in hogging condition

FIGURE 2-2

TIME	CYCLES
1 hour	$12X10^3$
1 day	$288X10^3$
1 week	$2X10^6$
1 month	$8.6X10^6$
1 year	$103X10^6$
30 years	$3110X10^6$

Cyclic loading rates for a misaligned shaft operating at 200 rpm.

TABLE 2-2

platforms the strength of the shaft or bearing placements may need to be over designed to withstand the loading fatigue instigated by forces external to the equipment. While bearing-shaft alignment problems may not show up in vibrational analysis techniques their importance cannot be ignored. It is important to note that axial bearing alignment is essential in preventing bearing damage, but also in preventing failures due to fatigue. In cases where shaft-bearing alignment cannot be maintained due to placement on moving platforms shaft strength over design should be utilized to prevent failures.

2.2 BOWED ROTORS

For varieties of reasons single shafts are often operated which when unsupported are not axially in line. These shafts or rotors are said to be bowed. A bowed rotor may be the result of incorrect manufacturing, incorrect installation or improper operation. However, in all cases the bowed rotor phenomenon shows up in vibrational analysis as a one times rotating speed spike. (see figure 2-3). These one times rotational operating speed spikes are indicative of two types of bowed rotor phenomena. The first case being a bowed rotor supported by axially in line bearings. The second type of bowed rotor phenomena occurs when a bowed rotor is forcefully aligned in axially concentric journal bearings.

For a shaft bent such that the centroid of mass of the rotor does not lie on the axis of rotation is analytically the same as an unbalanced rotating disk. These configurations can be seen in figures 2-4a and 2-4b. A rotor can be bowed for a variety of reasons. In steam turbines improper heating or cooling of the rotor will leave a residual bow, poor fitting of rotating elements could cause permanent offset or

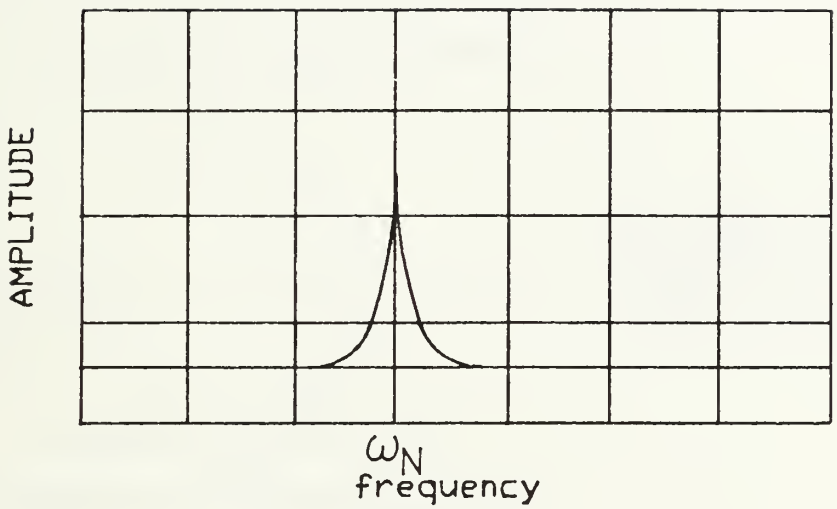

Spectra showing one times rpm vibrational spike.

FIGURE 2-3

Bent shaft in aligned bearings

(a)

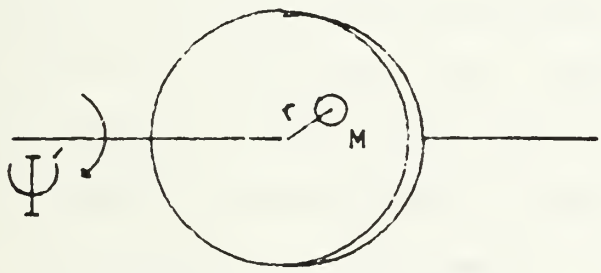

Unbalanced rotating disk

(b)

Bent rotor placed in axial aligned bearings is similar in analytic characteristics as an unbalanced rotating disk

BENT ROTOR BEHAVIOR WHEN PLACED IN AXIALLY ALIGNED BEARINGS.

FIGURE 2-4

poorly manufactured shafts can be axially unsymmetric. In all cases the unbalanced shaft can be modeled as a rotating disk with an element whose centroid does not coincide with the shaft axis of rotation. This unbalance is represented by a centroid of mass "M" with off-set "r" in figure 2-4b. Therefore, as the shaft rotates at operating speeds, shaft or machinery vibrations exist. Using a FFT spectrum analyzer and an accelerometer oriented radially from the shaft, a spike coinciding with the machine operating frequency can be seen. By marking the shaft with light reflecting tape to establish the key phasor and using an optical sensor the FFT spectrum analyzer can be used in such a way to determine the phase relationship of the shaft bow or unbalance with respect to the key phasor. Figure 2-5 shows this simple test set-up. The transmitted vibrational force which results from the shaft unbalance has been extensively analyzed by Dimentberg (1961) and Nichols (1976). It was shown that a rotating unbalanced disk on a simply supported shaft exhibited a vibrational magnitude dependent on the disk mass, radial offset from the rotating axis and rotating angular velocity squared. This relationship is shown in equation one.

$$F = MC\ \omega^2\ )r \qquad (1)$$

It should be noted that the fluctuating vibrational force is

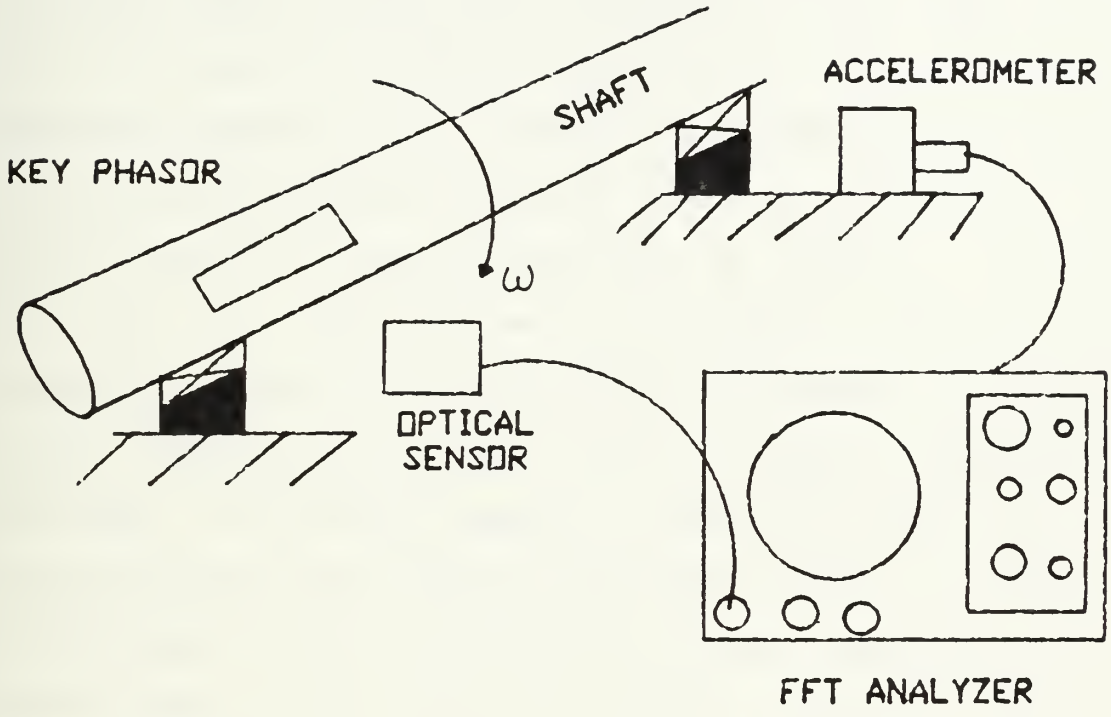

Test set up for determining phase relationships of a bowed or unbalanced rotor.

FIGURE 2-5

strongly dependent on the angular velocity. Quite clearly, the vibrational force increases rapidly in magnitude as the operating angular frequency is increased.

The second type of bowed rotor phenomena is the case of a bowed rotor being forcefully aligned in a set of axially concentric journals. In this case forces sufficient to bend the shaft to an axially aligned position are exerted by the bearing journals. This configuration is shown in figures 2-6(a and b). Once forced into position the journal bearings physically hold the shaft alignment. In this aligned position the shaft is no longer dynamically unbalanced. The shaft exerts a reaction force on the journal bearings equivalent to the force needed to deflect the bent shaft into its axially aligned position. This bending force is then exerted radially outward from the shaft onto the journal bearing. Consequently, as the shaft rotates the force exerted by the shaft rotates circumferentially around the journal. This force remains constant since there is no longer an unbalance and is equal to the static deflection force described above. Therefore, the transmitted vibrational force will be equal to the static deflection force at all angular velocities and will not change in magnitude as a function of rotating angular velocity. Subsequently, for the case of the bowed rotor placed in axially aligned journals there will be a

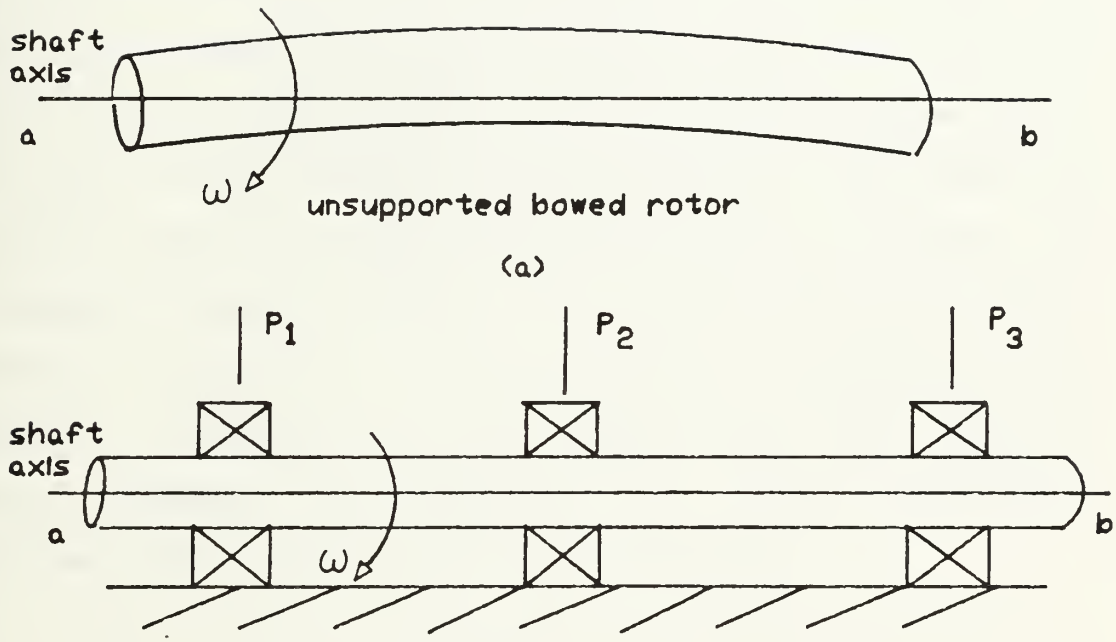
shaft
axis
a
b
ω
unsupported bowed rotor
(a)
P1
P2
P3
shaft
axis
a
b
ω
bent rotor forced into aligned journal bearings
(b)

FIGURE 2-6

vibrational force component of constant amplitude at frequencies corresponding to the system's operating angular velocity. It can now be seen that for the cases of bowed rotors there are two types of vibrational symptoms. In the case of the bowed or unbalanced rotor there is a force component whose magnitude increases as the square of the operating frequency. In the second case the physically aligned bowed rotor has vibrational force components of constant magnitude independent of angular velocity. In both cases the vibrations occur at frequencies corresponding to one-times the operating angular frequency. However, the two types of bowed rotor phenomena are discernible because for a bowed rotor placed between axially concentric bearings the resulting vibrational amplitudes increase as a function of the angular velocity squared. For the case of a bent rotor forcefully aligned in axially concentric bearings, the vibrational amplitude remains constant as the rotating angular frequency is increased (i.e. the vibrational amplitude is not angular frequency dependent).

Machinery operated with bowed rotors will always exhibit the one times rpm spike, but the practical consequences of the bowed rotor are more severe. As the rotor rotates inside its journals uneven or excessive bearing loading occurs. If this unsymmetrical loading is severe enough the oil film support can break down causing tribologic material failure

on the bearing surfaces, which in turn can lead to equipment catastrophic failure. In addition, rotation of the rotor outside its design orbit can cause collision of close tolerance components as in the vanes of steam and gas turbines leading to total destruction of the rotor and stator sections. Also, quieting is an important parameter and often times the mechanical vibration will exhibit a loud undesirable noise.

Today many equipments routinely operate at speeds in excess of many multiples of their rotors critical speed. As stated above a bowed rotor causes a forced vibration on the rotating system. When this vibration occurs at one of the resonant frequencies of the rotating shaft, large amplitude vibrations could result and lead to severe equipment damage. Therefore in high speed rotating machinery, rotor bow conditions due to a bent rotor forcefully aligned into axially concentric bearings or a bent rotor leading to unbalance must be minimized.

3.0 CONSTANT AND NON-CONSTANT VELOCITY COUPLINGS

In the previous sections problems associated with single rotor systems were discussed. The following sections of this paper will discuss vibrational problems associated with multiple rotor configurations. The connecting points in multiple rotor systems can give rise to a source of vibrational energy. Flexible couplings are often used to join the driving and driven ends of a multiple rotor system. A flexible coupling is a device used to transmit torque or power between two shafts which may or may not be co-linear. Although, gear and gear arrangement couplings fit into the definition of flexible couplings, they will not be treated in this study. In general couplings can be grouped into three basic categories; close-coupled, non-constant velocity couplings and constant velocity couplings.

3.1 CLOSE-COUPLED ROTORS

Close-coupled rotors consist of driving and driven rotors which are in theory axially aligned and rigidly fastened. Figure 3-1 shows an example of a hard coupled dual rotor set. This hard or close-coupled arrangement can tolerate

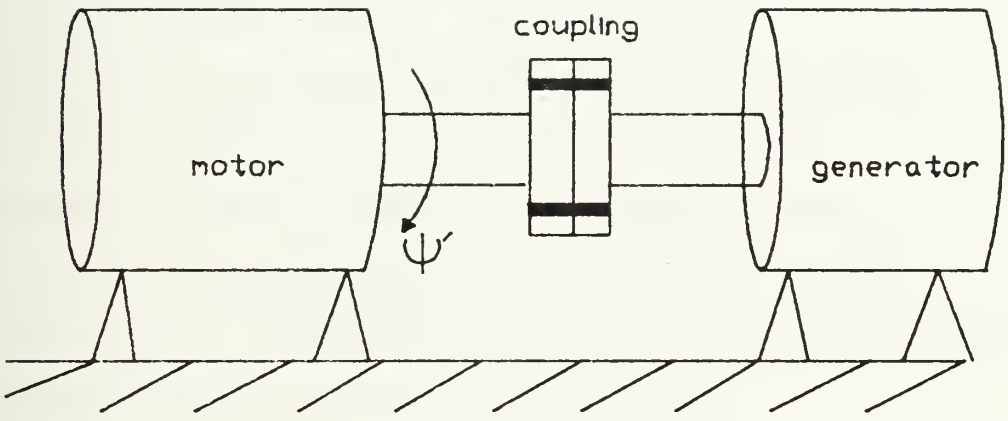

Close coupled motor-generator set.

FIGURE 3-1

very little mechanical misalignment. Either lateral or angular misalignment will result in skewing of the rotor combinations. Figure 3-2 (a and b) shows examples of lateral and angular misalignments. These undesirable misalignments will give rise to lateral vibrations at a frequency of one times the operating frequency which is similar to the bowed rotor vibrational frequency discussed earlier in this paper. In addition the closed coupled system must be accurately axially aligned to prevent damage to journal and thrust bearings. Therefore, close coupled devices are rarely used in major high-horsepower and high-velocity industrial equipment but rather are useful for low-power and low rpm operations or when exact alignments can be accomplished and maintained.

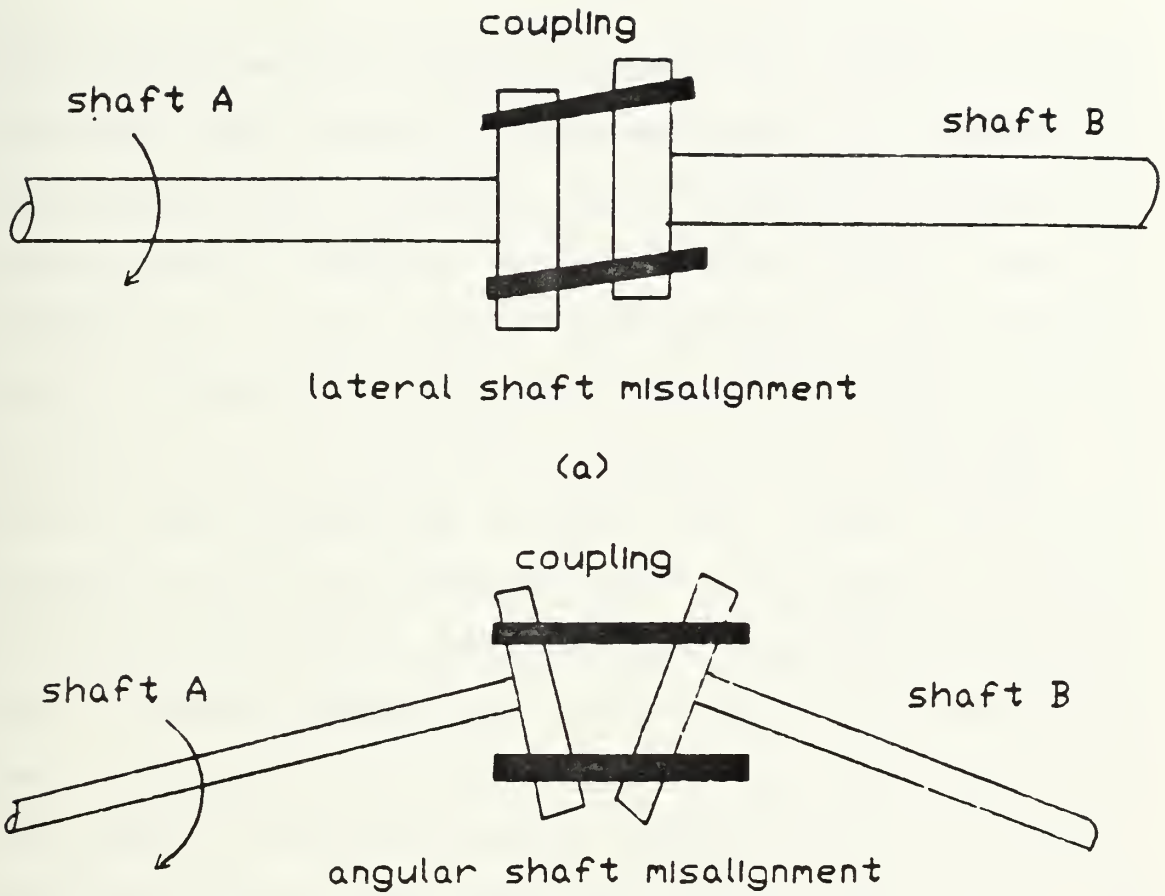
coupling
shaft A
shaft B
lateral shaft misalignment
(a)
coupling
shaft A
shaft B
angular shaft misalignment

FIGURE 3-2

3.2 NON-CONSTANT VELOCITY COUPLINGS

Non-constant velocity couplings are single element devices which when used to couple rotors can generally tolerate a significant amount of lateral and/or angular misalignment. A common type of flexible coupling which can be used to compensate or allow angular misalignments are universal joints (commonly called Hooke's Joints or Cardan Joints). As can be seen in figure 3-3 (a through c), a universal or Cardan joint consists of a drive yoke which is rigidly fastened to the drive shaft, a driven yoke which is rigidly fastened to the driven shaft and an orthogonal cross-pin which is used to connect the driving yoke to the driven yoke. The cross-pin is an orthogonal cross with each of its four members extending radially outward from the center. Opposite ends of each cross-pin member mate up to the driving and driven yokes. The ends of each cross-pin extend through sleeves on the respective yokes. This connection is similar to a shaft and journal junction. A mechanical fastener is then used to prevent the cross-pin from sliding free of the yoke. Once the yokes are attached to the cross-pin, the universal joint is assembled. In this assembled position each yoke is free to rotate about the axis of the yoke's attached cross-pin member. Due to the

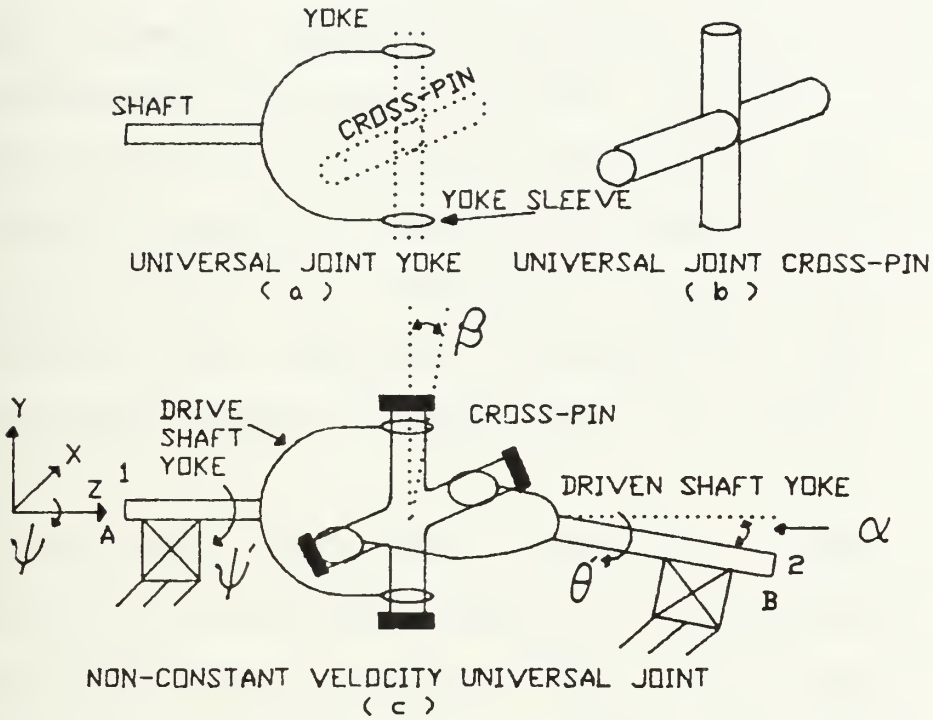

THE PLANE OF ROTATION OF THE CROSS-PIN FLUCTUATES BETWEEN POSITIONS NORMAL TO THE DRIVING AND DRIVEN SHAFT TWO TIMES PER DRIVE SHAFT REVOLUTION. THE ANGLE IS THE ANGLE SWEPT BY THE CROSS-PIN PLANE OF ROTATION.

FIGURE 3-3

orthogonal construction of the cross-pin, the planes of rotation of each of the yokes are orthogonal. It is the ability of the yokes to rotate about their respective cross-pin members which provides the universal joint flexibility. The universal joint is a flexible coupling which transmits torque and angular velocity with a mean transmission ratio equal to unity. However, the coupling when not in an axial aligned position does not transmit a constant velocity of rotation throughout each cycle of the driving rotor. In addition to being non-constant in velocity this asymmetric configuration gives rise to vibrations at even multiples of the rotating frequency.

In the double rotor system joined by a single universal joint, the non-constant velocity terms arise from the fact that the cross-pin does not remain in the constant bisecting angle plane for the entire angular displacements of one revolution. Since the respective yokes rotate about the cross-pin members to compensate for the misalignment, the plane in which the cross-pin lies fluctuates between positions normal to the driving and driven shaft two times per shaft revolution. In figure 3-3, β depicts the angular range of positions for planes in which the cross-pin moves throughout each revolution of the driving shaft (shaft 1). Shaft 2, the driven shaft, is displaced from the horizontal by angular displacement α . The relationship of the driving

to driven shaft angular velocities was investigated by Ota (1984a) and explained below. In figure 3-4 the vectors $\overline{p(\Psi)}$ and $\overline{q(\Theta)}$ are vectors from the cross pin center through the individual drive shaft yoke sleeves. The vector $\overline{p(\Psi)}$ extends outward from the universal joint cross-pin through the yoke sleeve of the driving shaft. The vector $\overline{q(\Theta)}$ extends outward from the coupling cross-pin through the yoke of the driven yoke. The coordinate system of figure 3-4 shows that the z axes coincides with the shaft axes, the x axes are normal to the z axes but in the same plane. On the other hand, the y axes are normal to the plane defined by the x and z axes. The position vectors $\overline{p(\Psi)}$ and $\overline{q(\Theta)}$ are represented by equations (1) and (2). It should be noted here that the yokes of the driving and driven shafts are displaced angularly by ninety degrees to properly mate with the orthogonal cross-pin.

$$\overline{p(\Psi)} = \cos(\alpha)\cos(\Psi)i + \sin(\Psi)j + \sin(\alpha)\cos(\Psi)k \qquad (1)$$

$$\overline{q(\Theta)} = -\sin(\Theta)i + \cos(\Theta)j \qquad (2)$$

Due to the shaft misalignment, the plane of rotation of $\overline{p(\Psi)}$ is not parallel to the plane of rotation of $\overline{q(\Theta)}$. However, if the misalignment angle was set to zero it is readily apparent that the $\overline{p(\Psi)}$ and $\overline{q(\Theta)}$ rotation planes would be parallel. Since $\overline{p(\Psi)}$ and $\overline{q(\Theta)}$ are vectors corresponding

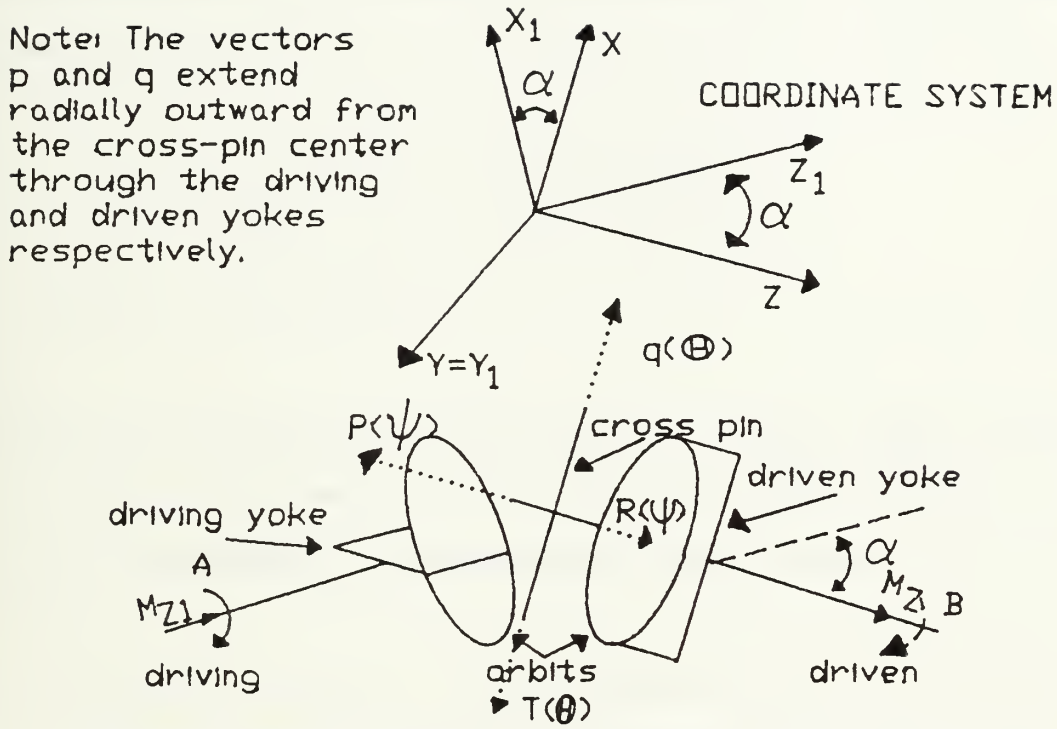

NON-CONSTANT VELOCITY UNIVERSAL JOINT COUPLING

FIGURE 3-4

to orthogonal cross pin members the scaler product of the two vectors must be equal to zero as in equation (3).

$$\overline{p(\Psi)} \cdot \overline{q(\Theta)} = 0 \qquad (3)$$

Inserting equations (1) and (2) into equation (3) yields the following results:

$$-\cos(\alpha)\cos(\Psi)\sin(\Theta) + \cos(\Theta)\sin(\Psi) = 0$$

$$\sin(\Theta)/\cos(\Theta) = \sin(\Psi)/(\cos(\Psi)\cos(\alpha))$$

$$\tan(\Theta) = \tan(\Psi)/\cos(\alpha) \qquad (4)$$

Projecting the plane of rotation of the driven shaft yoke onto the plane of rotation of the driving shaft yoke, the following trigonometric relationships are derived.

$$\sin(\Theta) = \sin(\Psi)/[1 - \sin^2(\alpha)\cos^2(\Psi)]^{1/2} \qquad (5)$$

$$\cos(\Theta) = \cos(\alpha)\cos(\Psi)/[1 - \sin^2(\alpha)\cos^2(\Psi)]^{1/2} \qquad (6)$$

Assuming that there is no friction between the cross pins and the yokes of the driving and driven shafts, the conservation of energy requires the moment that the drive shaft yoke impinges on the coupling cross pin is the same as the moment that the cross pin exerts on the driven shaft yoke. As previously explained the cross pin plane of rotation continuously alternates between positions perpendicular to the driving and driven shaft centers of

rotation two times per shaft revolution. The moment transmitted by the coupling cross pin remains normal to the plane of rotation of the cross pin. Therefore, as the cross pin rotates the plane of rotation fluctuates as does the normal to the rotating plane. The vector expressing the transmitted moment can then be written as some scaler times the cross product of the position vectors, $\overline{p(\Psi)}$ and $\overline{q(\Theta)}$, as seen in equation (7).

$$\bar{M} = M[\overline{p(\Psi)} \times \overline{q(\Theta)}] \qquad (7)$$

As mentioned above this moment vector does not continuously coincide with the axis of either the driving or driven shaft but rather oscillates between positions coinciding with the shaft axes two times per driving shaft revolution. Inserting equations (1) and (2) into equation (7) and segregating the vector elements yields:

$$M_z = \bar{M} \cdot \hat{k} = MD \qquad (8)$$

$$M_q = \bar{M} \cdot \overline{q(\Theta)} = 0 \qquad (9)$$

$$\bar{M}_T = \bar{M} \cdot \overline{q(\Theta + \pi/2)} = M\sin(\alpha)\cos(\Psi). \qquad (10)$$

where

$$D = (1 - \sin^2(\alpha)\cos^2(\Psi))^{1/2}$$

Similarly for the driving shaft moments the components are:

$$M_{z_1} = \bar{M} \cdot \bar{k}_1 = M\cos(\alpha)/D \qquad (11)$$

where $\bar{k}_1 = \hat{k}\cos(\alpha)$

$$M_P = \bar{M} \cdot \overline{p(\Psi)} = 0 \qquad (12)$$

and

$$M_R = \bar{M} \cdot \overline{p(\Psi + \pi/2)} = -M\sin(\alpha)\sin(\Psi)/D. \qquad (13)$$

Equations (8) through (10) represent the transmitted moments. M_z is the moment transmitted along the driven shaft. Moment components M_α, M_T, M_P and M_R which are components corresponding to the cross pin to yoke combinations give rise to the observed lateral vibrations of a misaligned flexible coupling. For α equal to zero, these components are eliminated. To determine the non-constant velocity of the output shaft in this coupling arrangement the time derivative of the output shaft position Θ' needs to be resolved. Taking the time derivative of equation (3) yields:

$$(\overline{p(\Psi)} \cdot \overline{q(\Theta)})' = \Psi'\cos(\alpha)/D - \Theta'D. \qquad (14)$$

Substituting equations (8) and (11) into (14) yields:

$$(\overline{p(\Psi)} \cdot \overline{q(\Theta)})' = (1/M)[\Psi' M_{z1} - \Theta' M_z]. \qquad (15)$$

Since the coupling was assumed to be frictionless, the time rate of work of the drive shaft ($M_{z1}\Psi'$) must equal the time rate of work of the driven shaft ($M_z\Theta'$). This gives

rise to the following:

$$\Psi' M_{z_1} = \Theta' M_z. \qquad (16)$$

Solving for the drive shaft angular velocity yields:

$$\Theta' = \Psi' \cos(\alpha) / (1 - \sin^2(\alpha)\cos^2(\Psi)). \qquad (17)$$

Where Θ' is the angular velocity of the output shaft. Therefore, equation 17 expresses the input-output angular speed relationships for misaligned flexible couplings.

Universal joints can be constructed to allow variations in angular misalignments of up to 45 degrees. Investigating equation (17) in some detail will yield some interesting results. For $\alpha = 0$ the driving and driven angular velocities are equal and constant with respect to position. Therefore, when there is no angular displacements the coupling arrangement is said to be a constant velocity coupling (i.e. $\Theta' = \Psi'$). The cases of constant velocity couplings will be discussed in following sections.

When α is fixed at some constant value it is readily apparent that the driven angular velocity (Θ') is a function of the driving angular displacement (Ψ). For example if α = 10 degrees and the driving velocity is 30

cps equation (17) becomes:

$$\Theta' = 29.54/(1 - .030\cos^2(\Psi)).$$

Table 3-1 shows the various rotational speeds of the driven shaft as a function of angular displacement of the driving shaft. Using the reference for Ψ in figure 3-3, it can be seen that velocity is minimum when $\Psi = \pi/2$ or $3\pi/2$ and maximum when $\Psi = 0$ or π. Therefore, an angular velocity maximum occurs each time a plane occupied by the cross pin of the universal joint is perpendicular to the driving rotor or when the cross pin plane is perpendicular to the driven rotor. Minimum velocities occur when the connecting point plane swept angle (β) of figure 3-3 is bisected. Consequently, for each driving shaft revolution there are two minimum and two maximum angular speed variations.

These two times shaft rpm oscillations of the cross pin also correspond to the forces and moments generated as the cross pin moves alternately from positions perpendicular to the driving shaft to positions perpendicular to the driven shaft as shown in equations 8 through 13. Ota (1984a) in his analysis of the single non-constant velocity coupling decomposed the rotor force and moment fluctuations into their respective x and y components. These equations are listed below:

Ψ (deg)	(30cps)	(cps α = 10 deg)	(cps α = 30deg)
00	30	30.46	34.46
45	30	30	29.7
90	30	29.54	25.98
135	30	30	29.7
180	30	30.46	34.46
225	30	30	29.7
270	30	29.54	25.98
315	30	30	29.7
360	30	30.46	34.46

Driven shaft angular velocities as a function of driving shaft angular displacement and driven shaft misalignment.

TABLE 3-1

$$F_x = (-3/(4a)\tan(\alpha)\sin(2\omega t))[(1 + 2\sum_{N=2,4,6\ldots}^{N/2}\varepsilon\cos(N\omega t))$$
$$(M_b - \delta_t\sum_{N=2,4,6\ldots}^{N/2}\varepsilon d_n\sin(N\omega t))] \quad (18)$$

$$F_Y = (3/(4a)\sin(\alpha))(1 + \cos(2\omega t))[(1 + 2\sum_{N=2,4,6\ldots}^{N/2}\varepsilon\cos(N\omega t))$$
$$(M_b - \delta_t\sum_{N=2,4,6\ldots}^{N/2}\varepsilon d_n\sin(N\omega t))] \quad (19)$$

$$M_x = aF_Y/3 \quad (20)$$

$$M_Y = -aF_x/3 \quad (21)$$

$$d_n = (2NI_p\omega^2)/(\delta_t - I_p(N\omega^2)) \quad (22)$$

and

$$\Psi = \omega t. \quad (23)$$

In equations 18 thru 21 M_b denotes a constant resisting moment acting on the driven shaft end (point B), " a " represents the distance from the driving end moment (point A) to the coupling centroid, δ_t corresponds to the rotors torsional spring constant and ε is a coefficient characteristic of the joint angle. The point being that these equations readily show the force and moments components to have even multiples of the driving frequency. These in turn give rise to the even multiple lateral vibrations observed when examining a skewed two rotor system coupled by a single universal joint.

The above vibrational phenomenon is often used in determining rotor axis alignment in rotating machinery. As

can be seen by equations 18 thru 21, the fluctuations in the transmitted forces and moments go to zero as the alignment angle α goes to zero. In addition, the vibrational magnitude increases as α increases. Use of these facts allows one to determine if rotating systems are aligned and also the degree of misalignment can be determined if any is present.

3.3 CONSTANT VELOCITY COUPLINGS

A constant velocity coupling in contrast to the non-constant velocity coupling discussed in the previous sections has a driven shaft speed always equal to the driving speed. A number of conditions are required to achieve this constant velocity. These conditions or criteria can best be seen by analyzing the simple shaft coupling arrangement of figure 3-5. In figure 3-5 each shaft has an arm bent at an angle β with the shaft centerlines displaced by an angle α. Depending on the actual coupling design, the flexible coupling may be constant velocity for a particular angle, range of angles or all angles. When shaft 1 in figure 3-5 is rotated the driving and driven shaft connecting point (A) rotates in a plane described by the coupling orbit. In figure 3-5 the shafts lie in a plane perpendicular to the plane defined by the orbit of the shaft coupling. The line of intersection of these two planes is represented by the line (A-A') of figure 3-5. Unlike the non-constant velocity coupling connecting plane, this plane of contact between the driving and driven shafts does not oscillate in the plane defined by the shafts but rather remains fixed throughout each shaft revolution. Although, the connection point "A"

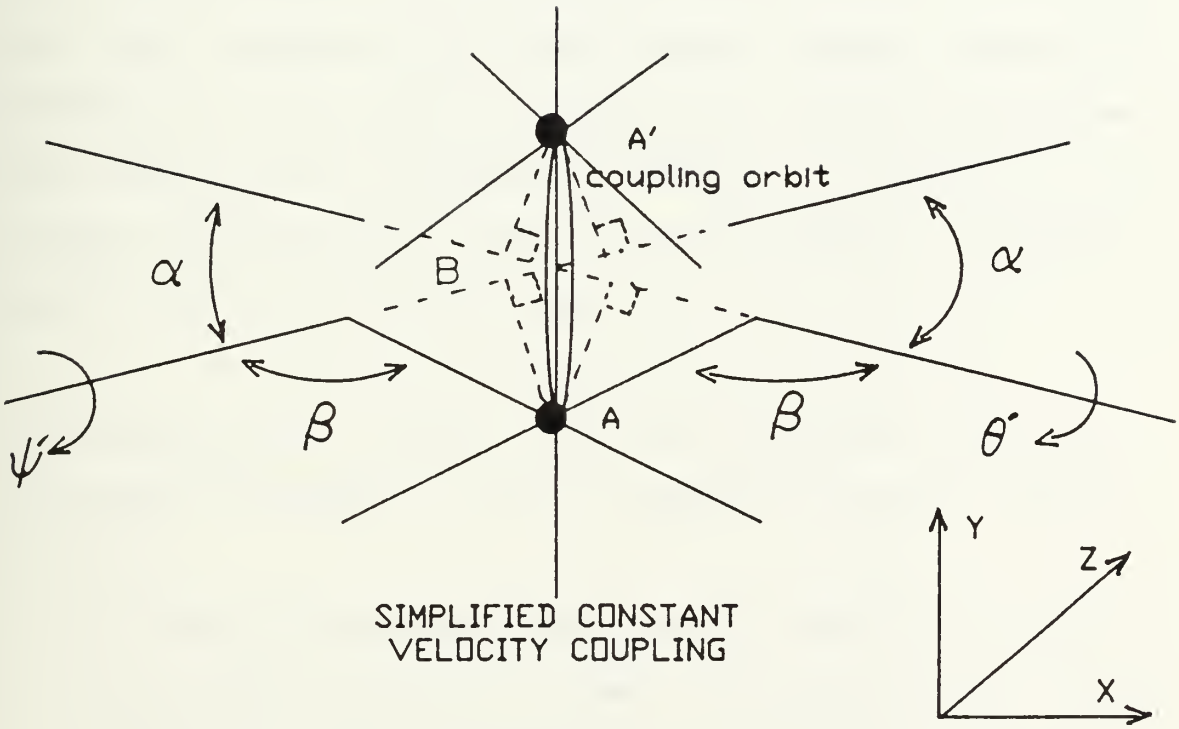

SIMPLIFIED CONSTANT
VELOCITY COUPLING

FIGURE 3-5

moves axially along the shafts as the shafts rotate, the perpendicular line segments from the shaft connecting point (A) to shafts 1 and 2 remain equal in length. Therefore, the radii from the rotating shafts to the rotating point "A" is the same for both shafts. As the driving shaft rotates through each revolution, the connecting point (A) continually lies in the fixed plane defined by the coupling orbits. In this constant plane of rotation, point A remains at an equal radius of rotation (A-B) for both rotating members. Therefore, since the line segment A-A' remains fixed in space and the connecting point to shaft extension radii are constant for both shafts, simple geometric arguments show that the line segment A-A' bisects the obtuse angle formed by the misaligned shafts. In addition, the constant connecting point radii keep the angular velocities constant and equal at all times.

The examination of figure 3-5 has illustrated the four requirements necessary to have a constant velocity flexible coupling.

(1) The driving and driven shaft's plane of contact must remain constant in space throughout each shaft revolution. This is different from the plane of contact of a single universal joint which cycles between positions perpendicular to each shaft twice during each revolution.

(2) The plane of contact point rotation must remain normal to the plane defined by the rotating shafts.
(3) This plane of contact must exactly bisect the obtuse angle made by the offset shafts. (This bisected angle will be one-half of the total shafts obtuse offset angle.)
(4) While obvious for two shaft arrangements, for three or more shaft configurations all shafts must lie in the same plane.

A large number of constant velocity flexible couplings are currently available in the market place. They include ball couplings, tripot couplings, disk couplings and numerous arrangements of multiply connected universal joint couplings. Using the criteria laid out for a constant velocity coupling, a double universal joint coupling will be analyzed in the following paragraphs and a disk type constant velocity coupling will be analyzed in a latter chapter of this text.

Figure 3-6 depicts a three shaft - double universal joint constant velocity coupling arrangement. The total joint displacement angle is 2α . Shaft number 2 is the coupling yoke whose mid-point (C) constantly remains in the shafts plane of rotation. The first constant velocity coupling criteria is thus satisfied in that for each revolution this

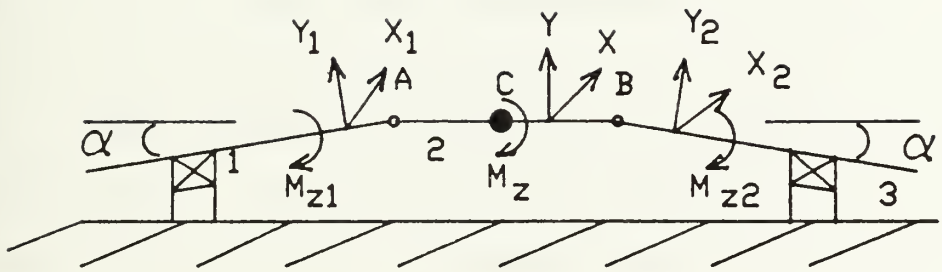

Three shaft double universal joint
constant velocity coupling

FIGURE 3-6

point of contact remains constant in space. Also, the plane of contact remains normal to the plane defined by the rotating shafts, which satisfies the second criteria for constant velocity couplings. It should also be understood that to be a constant velocity coupling all three shafts must lie in the same plane. Finally, geometric arguments show that at the number two shaft midpoint the rotating plane of contact bisects the angle formed by the offset shafts meeting the third requirement for constant velocity couplings. It should be emphasised that the symmetry shown in figure 3-6 is essential for constant velocity operation. Figure 3-7 shows some other configurations in which constant velocity coupling can be achieved with double universal joints. Again, keeping in mind that all shafts must lie in the same plane. A more subtle requirement for the double universal joint coupling to achieve constant velocity is the couplings yoke-cross pin arrangement, which will be discussed in the following section.

At this point it should be shown that in addition to an intuitive argument a mathematical argument holds for the constant velocity coupling. Recalling that the equation for the non-constant velocity coupling is a function of the shaft angular displacement, rotor position and driving shaft angular velocity, equation 17 of section 3-1 is repeated.

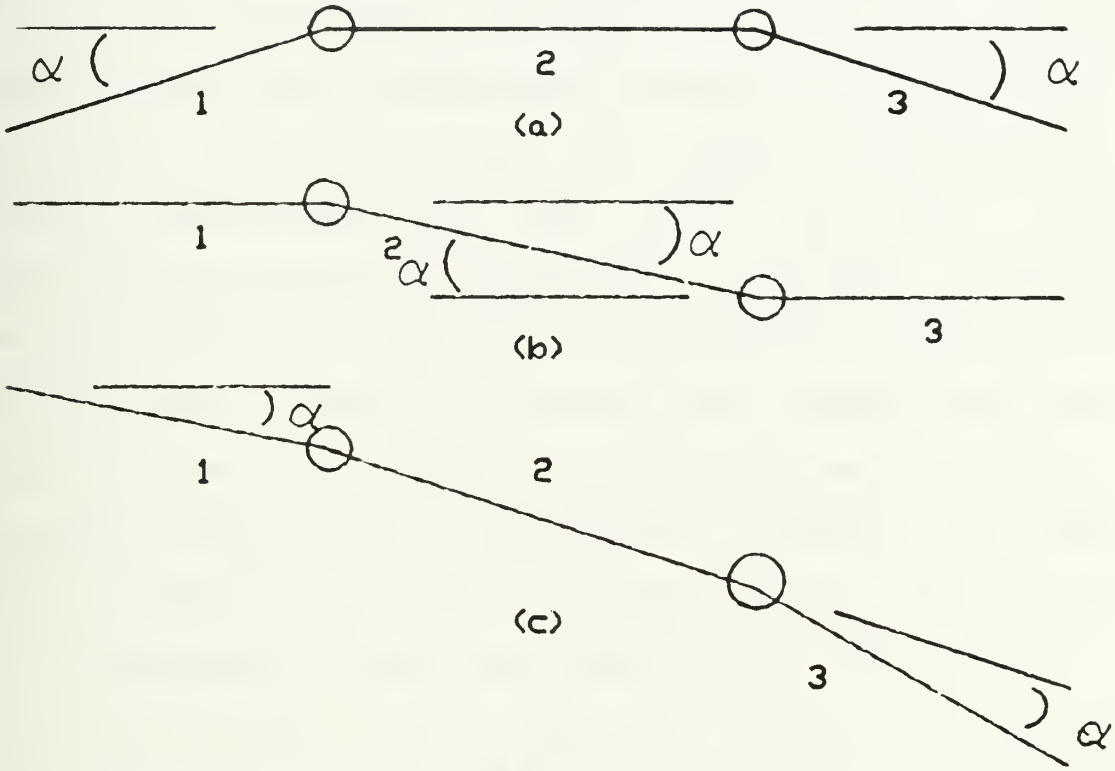

Constant velocity universal joint configurations

FIGURE 3-7

$$\Theta' = \Psi'\cos(\alpha)/(1 - \sin^2(\alpha)\cos^2(\Psi)) \qquad (1)$$

Applying equation (1) to shafts 1 and 2 of figure 3-6, it is apparent that shaft 2 does not rotate at constant velocity but rather at a speed specified by the non-constant velocity coupling equation. Also, for proper operation the yokes on shaft number 2 must be angularly aligned as in figure 3-8 with their respective cross pin members parallel. The velocity relationship for the shaft two and three combination of figure 3-6 can then be developed. Invoking the same procedures and assumptions outlined in section 3.2, the time rate of work of the driven shaft (shaft #3) must equal the time rate of work of the driving shaft (shaft #2). In essence there are two non-constant velocity universal joints joined by the common coupling shaft. The moment (M_{x1}) transmitted axially along the driving shaft must be equal to the moment (M_x) transmitted along the coupling shaft as shown in section 3.2 of this study. For the same reasons, the moment (M_{x2}) transmitted axially along the driven shaft (shaft #3) must also be equal to the moment (M_x) transmitted along the coupling shaft. Therefore, we have:

$$M_x = M_{x1} = M_{x2}. \qquad (2)$$

The time rate of work for each shaft must also be equal

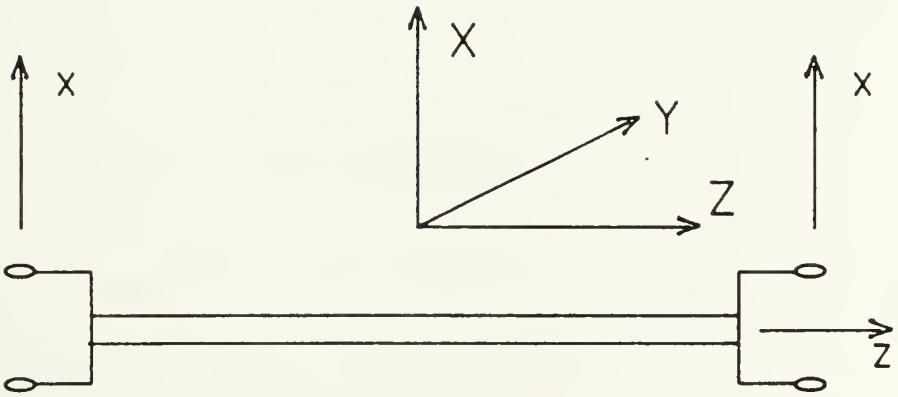

Coupling shaft yoke arrangement

FIGURE 3-8

(again assuming frictionless couplings) so that:

$$\Psi' M_{z1} = \gamma' M_{z2} \qquad (3)$$

Where

$$M_{z1} = M\cos(\alpha)/D \qquad (4)$$

and

$$M_{z2} = M\cos(\alpha)/D \qquad (5)$$

noting that

$$\Psi = \omega t$$

and

$$D = (1 - \sin^2(\alpha)\cos^2(\Psi))^{1/2}.$$

Inserting equations (4) and (5) into equation (3) then yields the constant velocity relationship:

$$\gamma' = \Psi' \qquad (6)$$

Consequently, it can be seen that the triple shaft double universal joint velocity relationship is a substantial improvement over the single universal joint design. Even though the coupling yoke (shaft 2) does not rotate at constant velocity, coupling shafts 1 and 3 do rotate at

equal constant velocities. As previously mentioned, the vectors normal to the cross pins oscillate between positions aligned with the center of rotations of the coupled shafts. It is these non-linear oscillations which give rise to the non-constant velocity phenomena as discussed in section 3.2 of this paper for single universal joint arrangements. Vibrations normally resulting from the shafts misalignments are eliminated in this double universal joint configuration. Even though coupling shaft #2 is not rotating at constant velocity and the rotational inertia of the shaft accelerate and decelerate twice during each shaft revolution, the acceleration components are out of phase with each other due to the coupling yoke arrangements and the force and moment generated vibrations have a cancelling effect. This cancellation yields a flexible coupling arrangement with constant velocity characteristics and without the two times angular velocity vibrations. The limiting factor in these joint designs is maintaining relatively small angles of angular displacement. In situations where more than 8 or 10 degrees of in plane angular displacement is desired the use of two or more of the double universal joint flexible couplings is an alternative. This configuration is shown in figure 3-9. However, in most applications where vibrational energy is a factor the angular misalignment is small and a single double universal joint flexible coupling is sufficient.

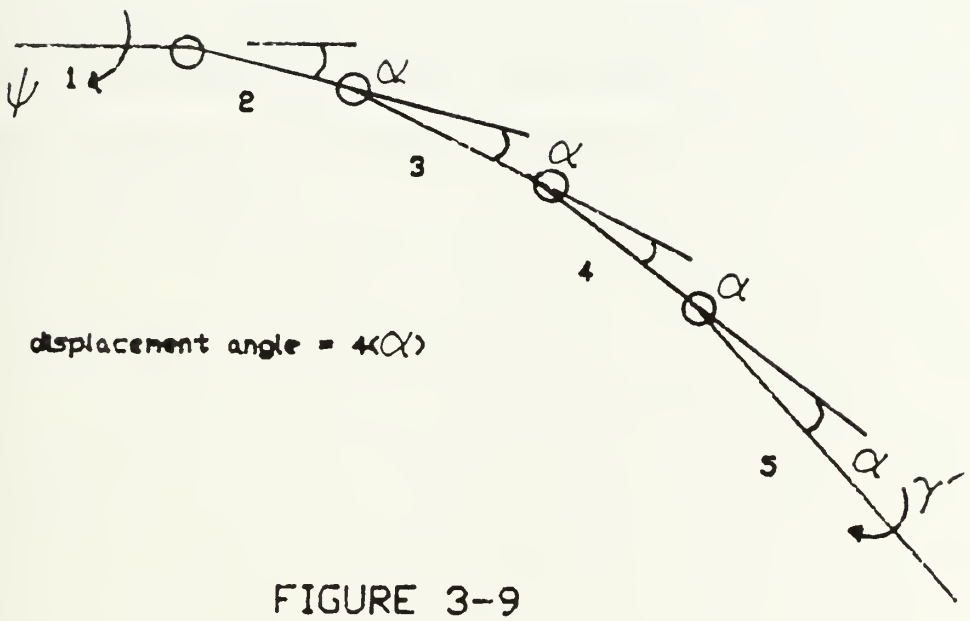

FIGURE 3-9

In summary the symmetry of shafts one and three of figure 3-5 is critical in achieving a constant velocity coupling. Once the shafts are aligned such that the symmetry is lost or the shafts are no longer in the same plane, the system is degraded to a system of two single universal joints. This gives rise to a non-constant velocity coupling and their components of vibrational energy at frequencies of multiples of two times the operating angular velocity. So once again the two times operating speed vibrations can be an indicator of misalignment in the double universal joint flexible shaft coupling arrangement.

4.0 RUBBER COUPLINGS

Although metallic flexible couplings including a variety of universal joint configurations are the most popular means of compensating for angular misalignment, rubber couplings are often used in applications where minimal shock loads, torsional vibration and noise transmission are desired. Due to the mechanical properties of rubber, these couplings are usually limited to relatively low torque applications. The applied torque of the driving shaft determines the size of the rubber coupling which will withstand the load. As the torque requirements increase the rubber coupling rapidly becomes excessive in size. Rubber couplings can be grouped into either constant or non-constant velocity flexible couplings. However, the constant velocity coupling is very limited in use due to very low torque applications. In addition rubber coupling behavior is a strong function of its Young's Modulus. This dependence on Young's Modulus is further complicated for rubber couplings due to the Young's Modulus dependence on rubber hardness, ambient temperature, geometry of the coupling, load frequency and load amplitude. Another disadvantage of the rubber coupling is its susceptibility to fatigue when cyclically loaded in both bending and torsion.

4.1 NON-CONSTANT VELOCITY RUBBER COUPLINGS

Rubber couplings when configured for non-constant velocity applications are similar to the previously described universal joint. However, in this case the cross pin is replaced by a rubber disk. Depending on the attachment geometry of the driving and driven shaft to the rubber coupling a non-constant velocity vibrational energy scheme of two or three times operating angular frequency can be observed for the unaligned shafts. If each shaft is connected to the rubber disk at two points the previously discussed two times operating speed vibrations will be observed. However, if each shaft is connected to the rubber disk by three connecting points vibrational energy will be observed at three times the operating angular frequency. Figure 4-1 shows a coupling arrangement very similar to the universal joint. For each revolution of the driving shaft a plane of rotation normal to the page and indicated by A-A' moves to positions normal to shafts one and two twice during each drive shaft revolution. As in the single universal joint previously discussed, this gives rise to non-constant velocity characteristics of the output shaft. This output velocity fluctuates between minima and maxima two times during each revolution of the driving shaft. In configurations using three shaft to rubber disk connecting

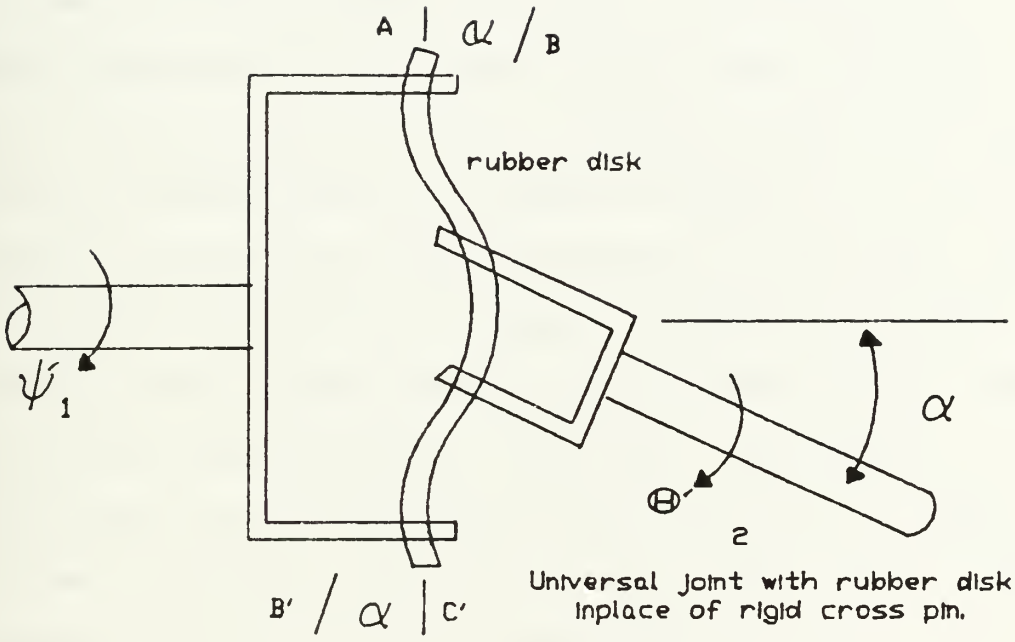
A
α
B
rubber disk
ψ1
α
2
B'
α
C'
Universal joint with rubber disk
inplace of rigid cross pin.

FIGURE 4-1

pins the same argument as above can be used to show that these speed excursions now happen three times per each revolution of the drive shaft.

Alternate cycling of the connecting disk between positions normal to each shaft leads to rapid fatigue of the disk when shaft angular displacements are large. For this reason the angular misalignment of a rubber disk type couplings is usually limited to small angles. In these cases the speed variations and the forces and moments generated are small. In addition the material characteristics of the rubber disk aid in transmitted force and moment vibration absorption. The bending and torsional movement of the disk absorb most of the energy generated due to the shaft misalignment. In addition noise transmission from the driving end rotor is effectively isolated from the driven end due to poor propagation properties of the rubber disk.

4.2 CONSTANT VELOCITY RUBBER COUPLINGS

Rubber couplings can be configured in a constant velocity mode. These flexible couplings allow a larger degree of angular misalignment but are usually limited to very low torque applications. Figure 4-2 shows a constant velocity rubber coupling. For steady rotating loads the shaft can be assumed to be torsionally rigid. In this case the driving and driven shafts operate at the same constant speed. For each rotation the rubber coupling alternately is loaded in tension and compression once again giving rise to possible rapid fatigue failure. For low torque and low rpm applications this constant velocity flexible coupling can be an effective means of transmitting torque through angularly misaligned shafts.

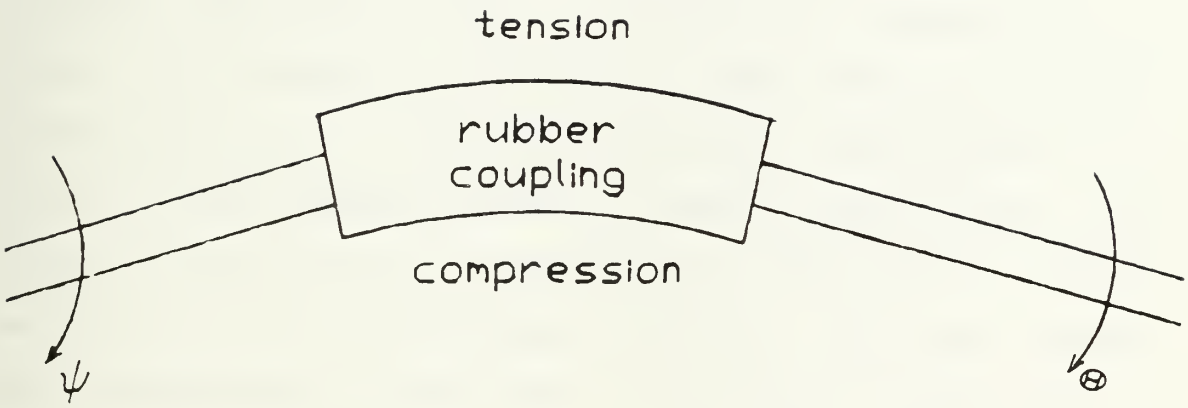

Constant velocity rubber coupling

FIGURE 4-2

5.0 SPLINES AND AXIAL MOTION DEVICES

In previous sections flexible couplings were used to account for angular and/or lateral misalignments when used in single or multiply connected combinations. With the exception of the rubber coupling which can withstand limited amounts of axial strain, axial motion and axial misalignment; axial motion could not be allowed. A spline is a flexible coupling which can be used to account or compensate for axial misalignment. As most of the previous flexible couplings could not compensate for axial misalignment, the spline cannot tolerate angular or lateral misalignment. The function of the spline is to transmit torque while allowing a degree of axial misalignment or motion. In some designs the spline may be configured to transmit torque but be permanently pinned so as not to allow axial motion. In this application the spline is used as an assembly aid in joining lengthy sections of drive shafts or rotors in interference laden environments. In still other applications the spline allows axial motion to exist during normal operating conditions. In the latter case the spline, as an axial motion compensating device, allows for length changes due to characteristics of the driving or driven mechanisms or vehicle motion geometries. Spline connecting geometries can

be lumped into two basic varieties, involute or parallel. An involute spline has teeth which have an involuted profile similar to that shown in figure 5-1. This design has high torque characteristics due to its strong tooth construction. The sides of the teeth of an involute spline act as drivers to transmit the torque (note the wide base of spline teeth). The major diameters of the spline may or not make contact depending on the spline-shaft fit characteristics while the minor diameters should not be allowed to make contact. Parallel sided splines are manufactured such that the driving teeth are parallel. The parallel tooth constructed spline does not exhibit as strong a torque characteristic as the involute spline of the same size, but is much cheaper to manufacture. An example of a parallel sided spline is shown in figure 5-2.

The spline coupling operates such that when torque is applied to the driving shaft it rotates into a position such that the sides of the teeth for the involute spline and the corners of the teeth on the parallel sided spline on the driving shaft end connection make contact with the sides of the teeth of the driven spline as shown in figures 5-1 and 5-3. In high torque applications this usually brings about rapid wear due to fretting in vicinity of the tooth contact points. In both of the above cases axial motion is compensated for by axial sliding of the spline teeth in the

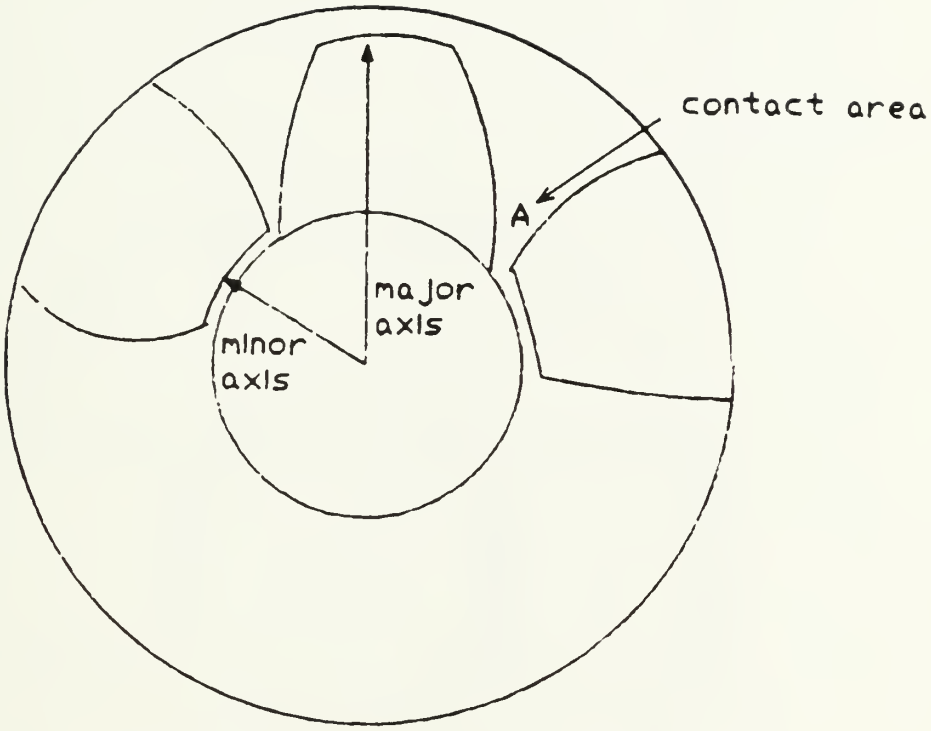

Involute spline tooth design

FIGURE 5-1

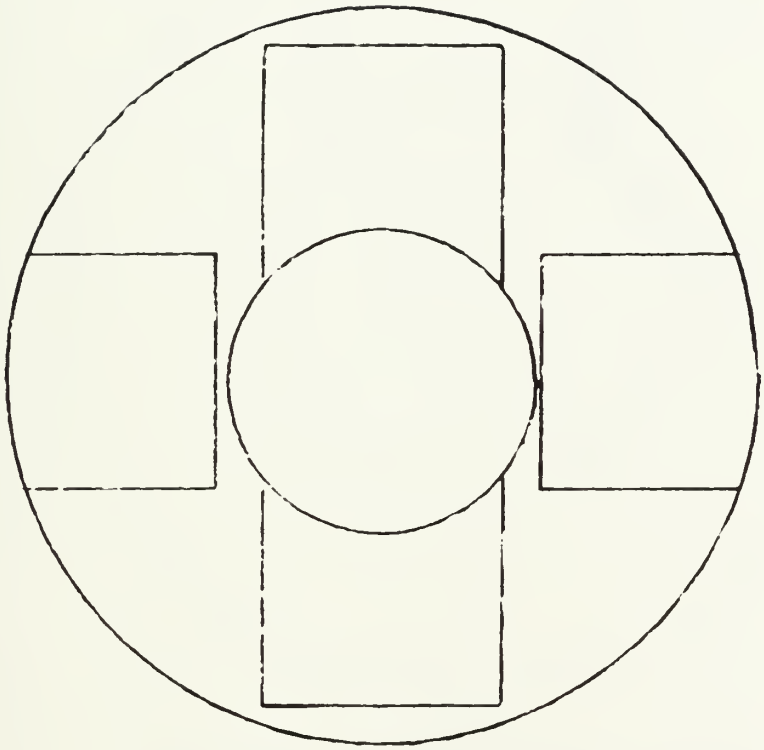

Parallel sided spline

FIGURE 5-2

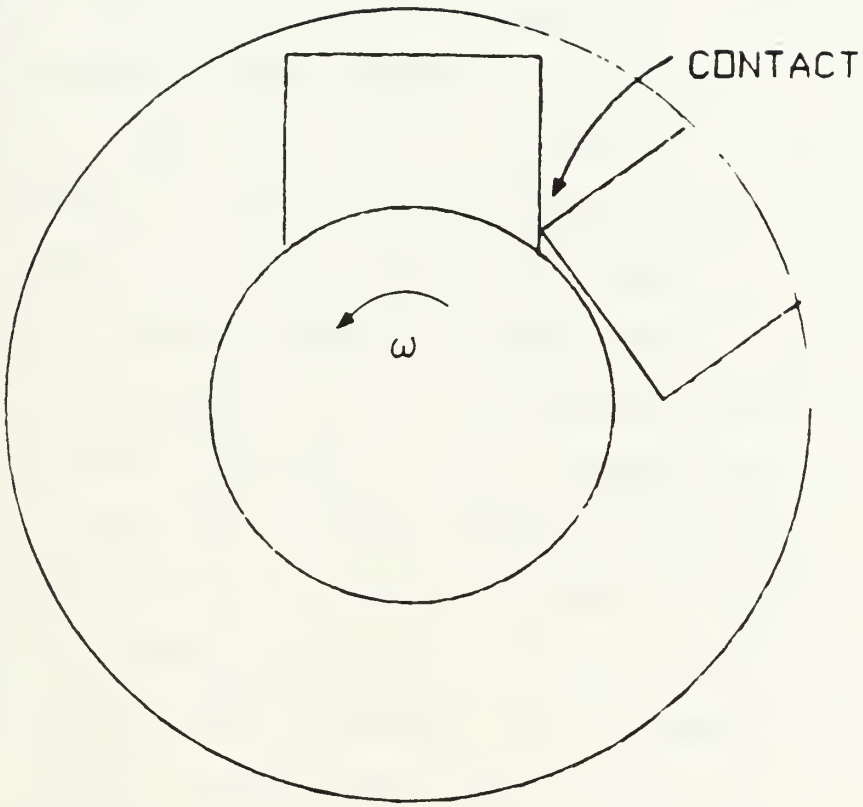

Parallel spline teeth contact

FIGURE 5-3

axial direction. In normal conditions this axial motion is smooth along the tooth contact. As the driving shaft rotates with some inherent axial motion tooth contact is maintained. The axial motion of the driving shaft is compensated for by increasing or decreasing the length of tooth contact within the spline. If properly designed and assembled the spline minimum length of contact should be greater than 0.8 times the spline diameter in order to maintain torsional strength of the coupling. In addition, if the spline surfaces are not properly lubricated the friction force between the tooth contact will be greater than the axial force and the spline will be essentially welded to the shaft allowing axial vibrations to be transmitted through the coupling. The fixed or pinned spline is generally used in applications in which the spline is used to allow easy assembly and disassembly, but when joined the spline is then pinned to prevent axial motion. Once assembled these splines no longer account for axial motion and will dynamically have the properties of a single rotating disk on a shaft.

To be properly operable the rotors joined by a spline must be axially aligned. If not properly aligned the spline coupling can exhibit either constant or non-constant velocity and vibrational characteristics. For the case of pure lateral misalignment as in figure 5-4 a non-constant

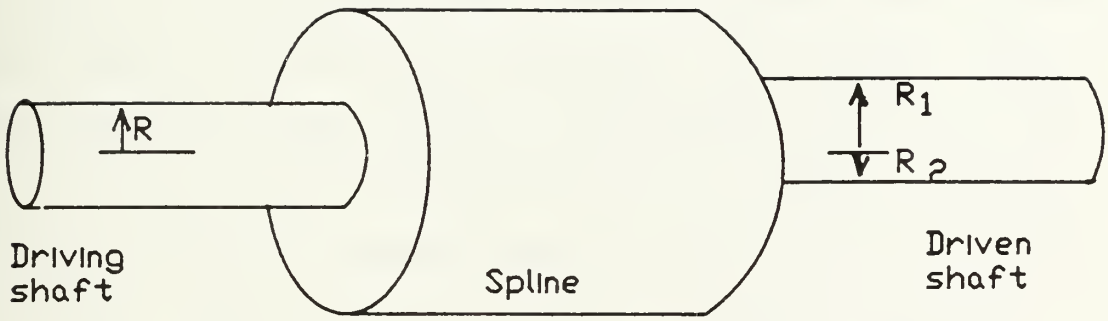

Spline coupled shaft with lateral misalignment.

FIGURE 5-4

velocity relationship will exist. This non-constant velocity characteristic arises from the fact that the radius of rotation of the driven shaft is not constant for all angular positions around its circumference. This assumes that there is sufficient play in the spline for lateral motion. If both shafts were pinned rigidly to the coupling the driven shaft would be forced to rotate in an orbit defined by the larger radius of rotation. For the non-constant velocity profile the maximum velocity occurs when R_1 is the radius of rotation and minimum velocity occurs when R_2 is the radius of rotation. In the case of pure lateral misalignment the speed maximum and minimum occur once per drive shaft revolution. For spline coupled shafts exhibiting pure angular misalignment as in figure 5-5, a constant velocity characteristic results. Assuming that the coupling is symmetrically fitted on the two shafts the rules required for constant velocity operation of section 3.3 of this paper can be applied. The shaft's plane of contact (defined by a plane intersecting the coupling in figure 5-5 and shown by line segment A-A') remains constant in space. In addition the rotating plane of contact remains normal to the plane defined by the shafts. Finally, in figure 5-5 the obtuse angle formed by the two shafts is bisected by the rotating plane of contact. The application of the constant velocity coupling criteria therefore shows that the spline with pure angular misalignment is a constant

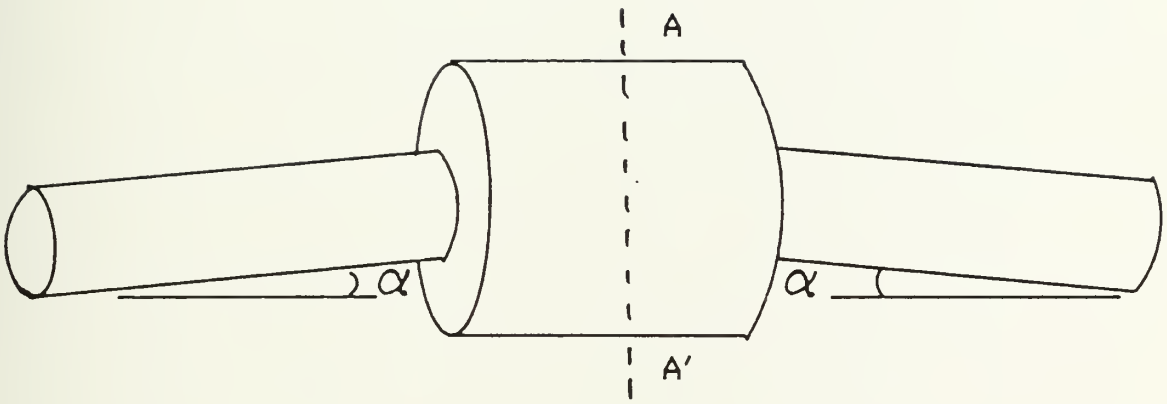

Spline coupled shaft with angular misalignment.

FIGURE 5-5

velocity coupling. In coupling combinations in which symmetry is not present or when combinations of misalignments occur the velocity profile will exhibit non-constant velocity characteristics.

5.1 DAMPING DUE TO SPLINE COUPLED SHAFTS

A more subtle but potentially more severe coupling situation occurs when a spline coupled shaft is operated in the rotors supercritical region. If not properly aligned and fitted the spline coupling could introduce internal damping to the rotating system. This internal damping is due to rubbing of the coupling on the shafts as relative motion between the shafts and coupling spline occurs while the shaft is rotating. Consequently, any disturbance introduced into the system which causes a bending action on the rotating element or deflection of the rotor to an orbit different than the normal spin about its axis will allow the damping mechanism to generate a force. In the subcritical regime the force generated by the internal damping mechanisms tends to stabilize the system and return the system to stable spin about its axis. A different situation arises when the rotational velocity is above the rotors resonant frequency. In this case the rotating angular velocity of the shaft is greater than the natural frequency of the rotor (i.e. supercritical). Introducing a shaft disturbance again causes a whirling action in which the shaft orbits in a path different from the spin about its axis of rotation. Depending on circumstances this whirl may be either in the direction of the driving angular velocity (forward whirl) or

in a direction opposite the driving angular velocity (backward whirl). If the interactions of the shafts and spline introduce an internal damping mechanism into the rotating system during a condition of forward whirl, instability could occur.

An explanation of the rotating shaft instability due to internal damping can be accomplished by energy methods as explained by Bucciarelli (1982). An energy transformation from kinetic energy due to spinning about the shaft axis to kinetic and potential energy due to the whirl orbit can be accomplished by internal damping introduced by the spline-shaft angular misalignment. The shafts and coupling spline can be modeled as in figure 5-6 where the spline-shaft rub has been modeled as a linear viscous damping and the spline mass as two rotating disks on separate shafts. In normal operation, the centers of mass of the disk lie on the axis of rotation. However, when a whirl state exists the shaft axis is displaced from the normal axis of spin by an amount described by the angle ( ) in figure 5-6. During this whirl orbit, relative motion between the rotor shafts and coupling spline introduce the damping modeled in figure 5-6.

Using Bucciarelli's (1982) model shown in figure 5-6, the internal damping mechanism, C_I, is modeled as linear

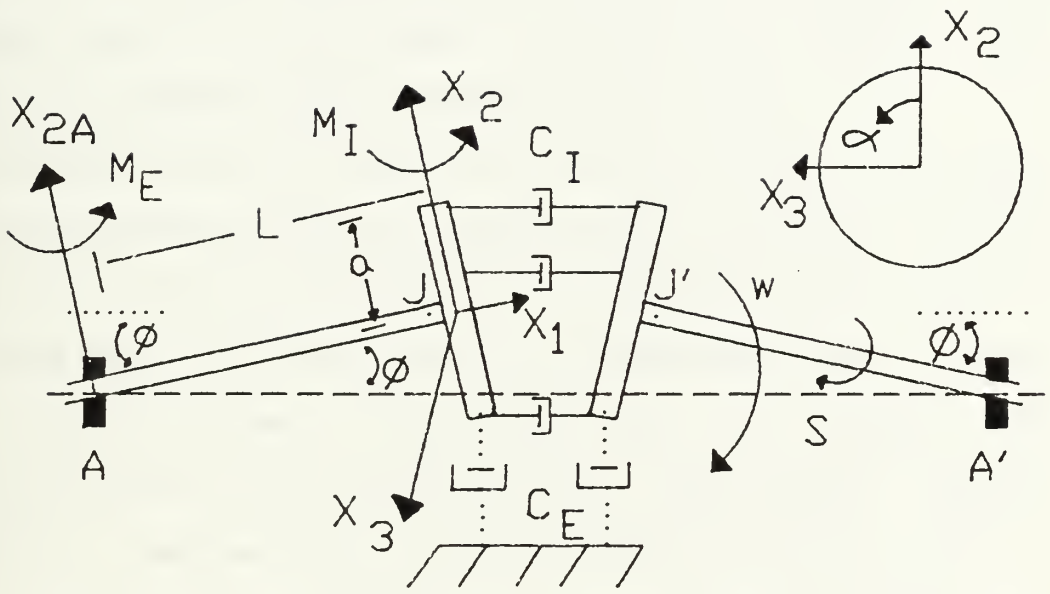

SPLINE COUPLED SHAFT MODEL

FIGURE 5-6

viscous damping distributed uniformly around the disks' outer circumferences connecting the two disks. An external damper, also distributed around the disks' circumferences, connects each disk to ground and is shown as C_E in the figure. This external damping acts to retard the motion of the shaft when in a whirl orbit. In order to isolate the potentially destabilizing elements of the shaft configuration shown in figure 5-6, an analysis of the forces and moments generated by the internal and external damping mechanisms must be accomplished. In figure 5-6, the normal spin axis of the rotating system is denoted by line segment A-A'. The displacement of the shaft from its normal spin axis is represented by the angle (ϕ). The shafts' angular velocity is represented by s and the whirl velocity by w. The X_1 axis lies along the shaft axis; and the X_2 axis originates at the center of the disk and extends radially outward as shown. (The X_1 and X_2 axes lie in the plane of the paper.) The X_3 axis originates at the disk center and extends radially outward from the paper. This coordinate system moves with the shaft as the shaft deflects away from its normal spin axis when whirling.

As the shafts whirl while spinning, the internal damping mechanisms generate forces which push and pull on the disk. The incremental force (i.e. force per unit radian) acting on the outer edge of the disk is defined as positive when

pushing outward on the disk and negative when pulling inward on the disk. The magnitude of the force generated by the internal damping mechanisms is a function of angular placement around the outer circumference of the disk (represented by the angle (α) measured from the X_{ie} axis) and the shafts displacement from its normal spin axis represented by the angle (ϕ).

The magnitude of the incremental forces generated by the internal damping mechanisms is dependent on the rate of longitudinal separation of the disks which in turn is dependent on the damping components angular location, (α), around the disks' outer circumferences. The longitudinal displacement due to the combination of whirl and spin is illustrated in figure 5-7. Figure 5-7(a) shows the end view of the disk. The disk center travels in the whirl orbit which has a radius Lsin(ϕ). Figure 5-7(b) shows the side view of the same disks. Note that L_o is the separation between the disks at their center for a fixed deflection angle (ϕ). Longitudinal separation at the top of the disk is L_o + 2asin(ϕ) and at the bottom the separation is L_o - 2asin(ϕ) as shown in figure 5-7(b). As the shafts whirl and rotate simultaneously, the point B on the outer circumference of disk of figure 5-7(a) deflects into the paper. The amount of deflection is function of angular position around the disk circumference denoted by (α).

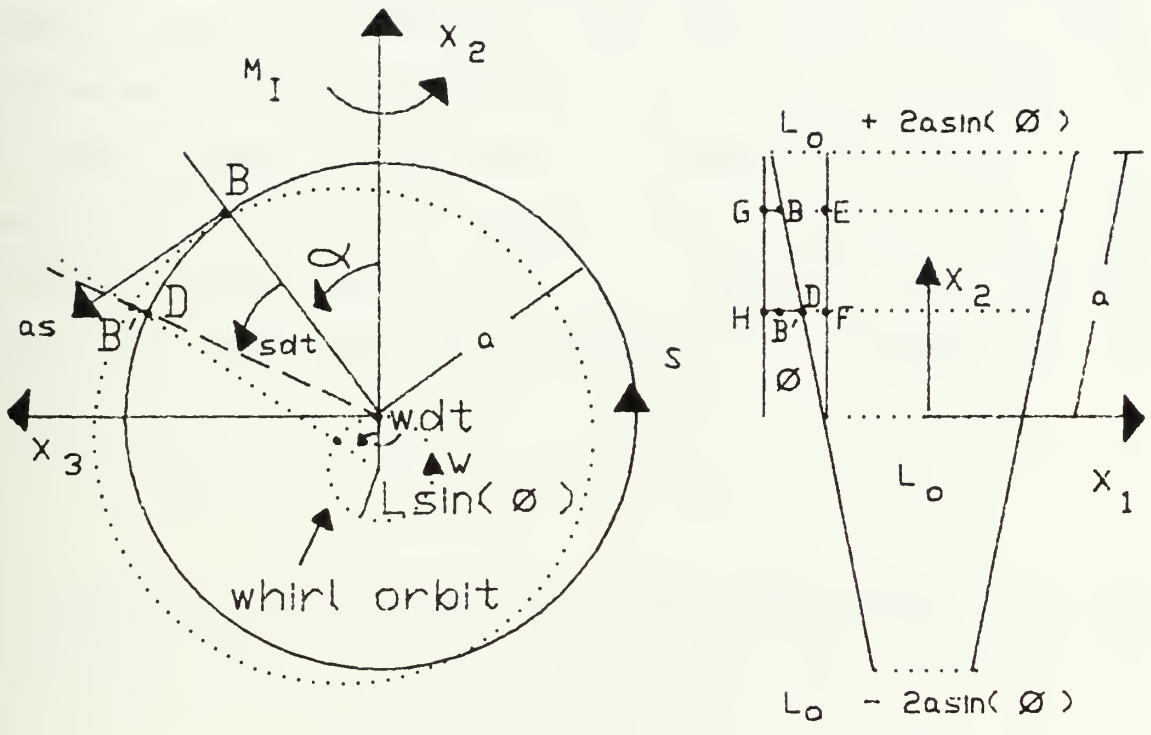

(a)
END VIEW

(b)
SIDE VIEW

ROTATING DISKS WITH SPIN AND WHIRL

FIGURE 5-7

The longitudinal deflection can best be visualized by first allowing the shaft to spin without whirling and then examining the shaft whirling without spinning. The longitudinal motion of the internal dampers due to spinning can by seen by fixing (ϕ) with a set of bearings located at points J and J' of figure 5-6. With the shafts held in their deflected positions (determined by (ϕ)), the shaft is allowed to spin. As the disk in figure 5-7 spins by an amount sdt, point B of figure 5-7(b) travels along the disk's circumference to point D. Therefore in the time period dt, the longitudinal change in disk separation is:

$$L_s = DF - BE,$$

as seen in figure 5-7(b). The longitudinal change in disk separation due to spin only can be written as:

$$\Delta L_s = L_o + 2a\cos(\alpha + sdt)\sin(\phi) - (L_o + 2a\cos(\alpha)\sin(\phi)$$

$$\Delta L_s = 2a\sin(\phi)[\cos(\alpha + sdt) - \cos(\alpha)], \qquad (1)$$

where $L_o + 2a\cos(\alpha)\sin(\phi)$ is the longitudinal displacement at point B. The sdt term represents the change in angular position around the disks circumference during an increment of time, dt. The longitudinal or axial velocity of the disk due to the change in angular position, sdt, is :

$$\frac{\Delta L_s}{\Delta t} = \frac{2a\sin(\phi)[\cos(\alpha + sdt) - \cos(\alpha)]}{dt} \qquad (2)$$

Invoking small angle approximations for sdt yields the longitudinal velocity due to the angular spin velocity to be:

$$V_s = -2as[\sin(\alpha)\sin(\phi)]. \qquad (3)$$

Equation (3) shows that as the disks spin, the disks' rate of longitudinal separation is negative. This agrees with figure 5-7(b) which shows the separation between the disks decreases when the disk spins from point B to point D.

To determine the longitudinal velocity due to whirl, the disks are not allowed to spin while the disks rotate about the A-A' axis in the whirl orbit of figure 5-6. As the point B of figures 5-7(a and b) rotates an amount wdt to point B', the change in longitudinal displacement of the disks is:

$$\Delta L_w = HD - GB,$$

which can be written,

$$\Delta L_w = L_o + 2a\cos(\alpha)\sin(\phi) - [L_o + 2a\cos(\alpha + wdt)\sin(\phi)]$$

$$\Delta L_w = 2a\sin(\phi)[\cos(\alpha) - \cos(\alpha + wdt)] \qquad (4)$$

This shows that as the shafts whirl about the A-A' axis by an amount wdt, the longitudinal displacement is increasing. Again invoking small changes in wdt yields:

$$\Delta L_w = 2a\sin(\alpha)\sin(\phi)\{wdt\} \qquad (5)$$

The longitudinal velocity due to whirl alone is then:

$$V_w = 2aw\sin(\alpha)\sin(\phi) \qquad (6)$$

The longitudinal velocity along the disk's circumference due to spin and whirl at a point defined by (α), (noting that (α) is measured with respect to the X_E axis), is:

$$V = V_w + V_s = 2a\sin(\alpha)\sin(\phi)[w - s] \qquad (7)$$

Now that the incremental forces, ($f = C_I V$), generated by the internal damping can be determined, the moment generated by the sum of the incremental forces can be written. The moment generated by the internal damping mechanisms, M_I, is

$$M_I = \int_0^{2\pi} C_I V(\alpha) a\sin(\alpha) d\alpha \qquad (8)$$

$$M_I = 2a\sin(\phi)(w - s)C_I \int_0^{2\pi} \sin(\alpha)a\sin(\alpha)d\alpha \qquad (9)$$

$$M_I = 2\pi a^2 C_I \sin(\phi)[w - s] \qquad (10)$$

where C_I is the damping per unit radian around the disks circumference. Equation (10) shows M_I to be stabilizing so long as $w > s$.

To complete the analysis, the effect of external damping needs to be determined. Figure 5-8 shows an end view of the disk with the external damping per unit radian, C_E, attached between the disks outer circumference and ground. The whirl radius is shown as:

$$\text{whirl radius} = r = L\sin(\phi). \qquad (11)$$

The radial displacement of the dashpots as the disk travels in the whirl orbit defined by equation (11) and shown in figure 5-8 is:

$$\delta = L_E - r\cos(\alpha) \qquad (12)$$

where L_E is the distance between the disk and ground when no whirl is present. In order to determine the radial component of the velocity due to the whirl velocity at a

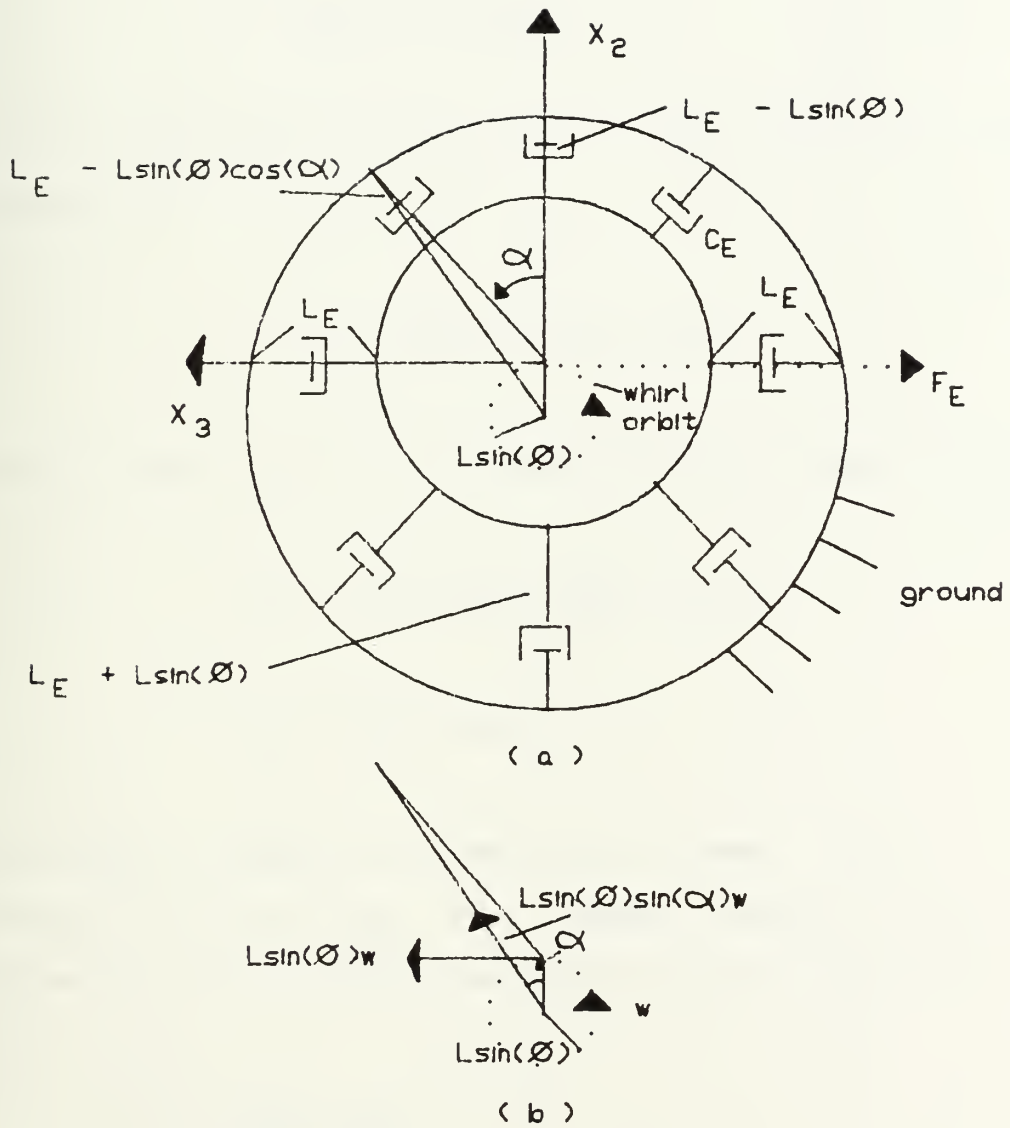

DISK END VIEW IN WHIRL

FIGURE 5-8

point on the disk's circumference, the components of the tangential whirl velocity need to be analyzed. Figure 5-8(b) shows the tangential velocity to be wLsin(ϕ). The radial component of that velocity is:

$$V_W = rw\sin(\alpha) \tag{13}$$

Thus the incremental force due to an individual damping element is:

$$f_E = rwC_E\sin(\alpha)\sin(\alpha)d\alpha \tag{14}$$

Summing these forces around the disk's circumference yields:

$$F_E = L\sin(\phi)wC_E \int_0^{2\pi}\sin^2(\alpha)d\alpha$$

$$F_E = \pi L\sin(\phi)wC_E \tag{15}$$

This force subsequently generates a moment about an axis parallel to the X_e axis and passing through point A of figure 5-6. This moment due to the external damping forces is:

$$M_E = LF_E \tag{16}$$

$$M_E = \pi C_E L^2 w\sin(\phi) \tag{17}$$

It should be noted that based on equation (17) M_E is always stabilizing.

Recalling that M_I is stabilizing when $w > s$, and that M_E is always stabilizing, stability requirements for the rotating system of figure 5-6 can be established. The system will remain stable so long as the sum of the moments acting on the rotating system are positive. Since M_I is a couple, the moments can be summed about the X_{ea} axis of figure 5-6. Therefore, the rotating system will be stable if:

$$M_E + M_I > 0. \tag{18}$$

Substituting equations (10) and (17) into equation (18) yields:

$$2a^2C_I[w - s] + L^2C_Ew > 0 \tag{19}$$

Consequently, the system is stable if:

$$2C_Ia^2s < (2a^2C_I + C_EL^2)w \tag{20}$$

and the system is borderline stable if:

$$s = [1 + C_EL^2/2C_Ia^2]w \tag{21}$$

In review, the internal damping components of figure 5-6 introduce forces into the rotating system which act on the shaft and generate a moment. This internal damping moment can be either stabilizing or destabilizing depending on the magnitude and direction in which it acts, (Recalling that the moment is stabilizing if: $w > s$.). On the other hand external damping applied on the rotating system retards the whirl orbit and is always stabilizing. Therefore, the external damping which is modeled in figure 5-6 by C_E is a stabilizing mechanism and internal damping modeled as C_I may be either stabilizing or destabilizing.

In backward whirl, the whirl orbit direction is in a direction opposite the shaft rotational angular velocity (i.e. w is negative). Therefore, the moment due to the internal damping and the whirl orbit acts in the same direction as the shaft's angular velocity and opposes the direction of the whirl angular velocity. Therefore, in backward whirl the internal damping will always have a stabilizing influence on the rotating system. In forward whirl, the moment due to the internal damping and the whirl orbit acts in the same direction as the rotating angular velocity and the whirl orbit (w and s are now both positive.). Therefore, rotating shafts operating with forward whirl may become unstable unless the criteria of equation (19) is met.

In summary, rotation in the subcritical angular velocity region and supercritical operation with backward whirl are conditions of stability. Shafts operating in the supercritical regime with forward whirl will be stable so long as:

$$s < [\,1 + C_E L^2 / 2 C_I a^2\,] w \qquad (22)$$

In all practical cases, the spline coupling must be angularly aligned such that the axial travel is limited to the design parameters of the coupling, lateral motion restricted and fitting parameters well suited for the particular application. Applications of the axial spline coupling devices are often in tandem with couplings designed to allow angular misalignment. For these compound couplings, shaft systems can be arranged to provide for angular, lateral and axial misalignments in either non-constant or constant velocity applications.

6.0 SHAFTS AND ROTORS

The preceding sections all assumed that system components were properly designed and installed to withstand the applied operating frequencies and load torques. There are several criteria in shaft construction and equipment arrangements which must be considered in order to prevent vibrational problems. The shaft construction and support arrangements must be adequate to support the work loads demanded. In addition, alignment criteria must be established and implemented on the rotating system which will take into account movement of the equipment foundations due to movement of the mounts and platforms, shock, and thermal expansion and contraction. In order to have a system of rotating elements operating properly and to achieve the equipment life expectancies, the system elements must be properly designed, the coupling devices properly selected and correct alignment criteria established and implemented. Rotating element design is a complicated issue which is a function of material properties, mounting configurations, application, applied torque, angular velocity and equipment size. In the following section a brief discussion is presented for two simply supported shaft designs. Equations similar to those presented are cataloged in various texts but each equation used must be tailored to the particular application.

Coupling devices have been devised for numerous applications. The coupling industry has thrived over the years with the number of coupling designs and sizes currently on the market ranging in the thousands. So rather than the design of a coupling being an issue, selection of the coupling from those available must accomplished. In chapter seven of this text, issues concerning coupling selection are discussed in detail. The discussion includes considerations which must be considered in general; and an analysis of a particular coupling is presented.

With shaft construction and coupling selection becoming an exact science, much remains to be determined concerning equipment alignment. The correct alignment procedures, alignment tools and allowable alignment tolerances are currently not agreed upon by most experts. In fact alignment techniques are often viewed as an art with the amount of misalignment tolerable left to the judgement of the mechanic or technician. In section 6.2 of this study a discussion is presented on two alignment techniques. Dial indicator methods which have been around since the turn of the century are briefly discussed and a "state of the art" laser-optical system operation is outlined. Finally, the issue of how much misalignment is tolerable in particular applications is discussed.

6.1 SHAFT CONSTRUCTION

For sections of circular shafts the design of the rotor must be sufficient to withstand the maximum applied torsional shear stress while minimizing the shaft angular twist per unit length. These values for circular shafts can be determined from equations (1) and (2) of this section.

Maximum torsional shear stress at the outer fiber:

$$S = 16Tdo/[(\pi)(do^4 - di^4)] \qquad (1)$$

Twist angle in radians/unit length:

$$\theta = 32T/[(\pi)(do^4 - di^4)] \qquad (2)$$

G = Torsional modulus of rigidity (psi)

T = applied torque (lb-in)

do = outer shaft diameter (in)

di = inner shaft diameter (in)

Torsional stiffness is important for a variety of reasons. A typical shaft can often be considered as a mechanism for connecting relatively large rotating inertias. This system can be subjected to a variety of vibratory excitations either forced or free in nature. Consequently, the drive

shaft or coupling shaft should be properly designed to retard shaft torsional vibrations. For instance the system resonant frequency can be altered by designing rotating element wall thicknesses to yield a desired torsional stiffness. Other parameters which may be varied to achieve desired system characteristics are shaft length, shaft diameter and rotating element material properties.

Another parameter which must be considered when designing coupling devices is the maximum rotating speed. This is particularly true for the double universal joint constant velocity coupling which makes use of several shaft sections. Whenever the shaft angular velocity approaches the shaft critical speed, vibratory oscillations can occur due to shaft whirling. The Critical speed of a rotating shaft is the same as the resonant frequency of the shaft in bending. Equations (3) and (4) define the critical speeds for <u>simply supported</u> solid and hollow rotating steel shafts with modulus of elasticity ($E = 29X10^6$) and density ($\rho = .281$ lb/in^3). These shaft configurations are shown in figures 6.1a through 6.1c.

Solid round shaft:

$$Nc = 4705000d/L^2. \qquad (3)$$

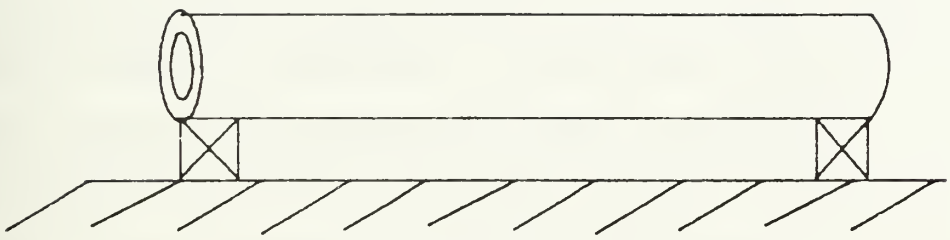

Simply supported shaft

(a)

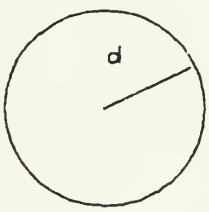

solid shaft

(b)

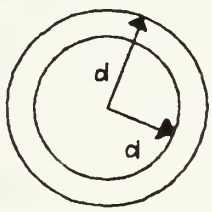

hollow shaft

(c)

SHAFT GEOMETRIES

FIGURE 6-1

Hollow round shaft:

$$Nc = 4705000(do^2 + di^2)^{1/2}/L^2 \qquad (4)$$

where: d = shaft diameter

di = inner shaft diameter

do = outer shaft diameter

L = shaft length

The coefficients of equations (3) and (4) are dependent on the end support conditions. Coefficients for a variety of shaft configurations and end support conditions have been catalogued in several texts (Den Hartog, 1956 and Harris 1961). Shaft systems quite routinely operate in frequency regimes above the critical speeds. However, operation near the critical angular velocities can yield vibrations corresponding to frequencies of the whirl velocities. In the case of forward whirl the whirl orbit is in the same direction as the rotating angular velocity; while backward whirl is in a direction opposite the applied angular velocity. These whirling cycles induce fatigue cycles which are substantially different. Figure 6-2 depicts a shaft whirl orbit with its accompanying stress cycle. As the shaft rotates counter-clockwise the whirl orbit is also counter-clockwise. Tracking the shaft whirl orbit through one cycle shows that the observed point goes through two stress maxima.

The frequency of the stress maxima in the forward whirl

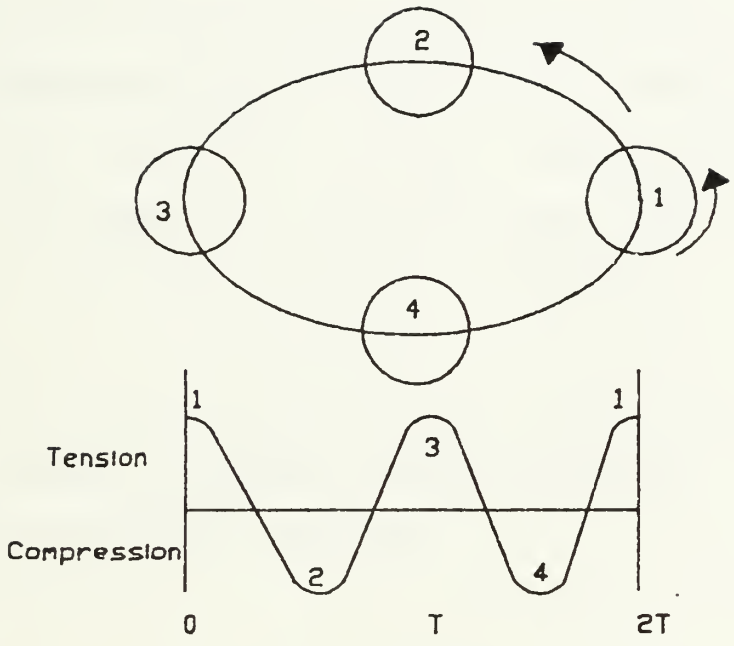

Fatigue Period
$T = 1/f = 1/(s - w)$

FATIGUE CYCLE FOR SHAFT IN FOWARD WHIRL.

FIGURE 6-2

state is the difference between the whirl velocity (w) and the shafts spin velocity (s) about its axis.

$$f_F = (s - w) \qquad (5)$$

When the whirl velocity is the same as the spin velocity, called synchronous whirl, there is no fatigue cycle and $f_F = 0$. As the whirl velocity deviates from the spin velocity in either the supersynchronous or subsynchronous direction, the fatigue frequency increases.

In backward whirl (shown if figure 6-3) the whirl velocity is in a direction opposite the spin velocity. The fatigue frequency of backward whirl is:

$$f_B = s + w. \qquad (6)$$

For a given whirl orbit the stress maxima are equal for both forward and backward whirl, but the occurrence of the stress maxima are much more frequent in the backward whirl case. Thus for fatigue loading the backward whirl case is much more severe given equal whirl orbits. Therefore, shaft specifications must be designed to prevent shaft whirl in order to prevent unwanted vibrations and to eliminate damage due to fatigue caused by bending action during the whirling cycles.

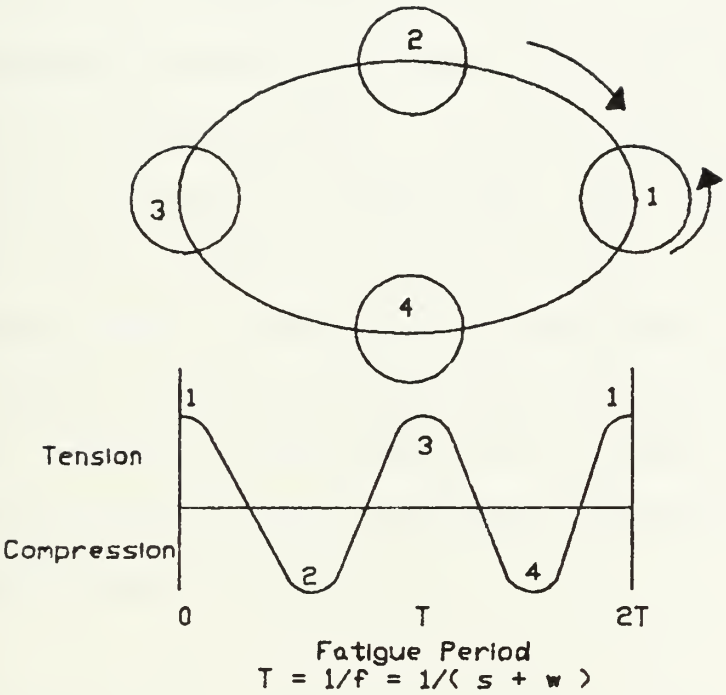

Fatigue cycle for shaft in backward whirl.

FIGURE 6-3

6.2 EQUIPMENT ALIGNMENT

Previous sections of this paper discussed the use of flexible couplings to compensate for misalignments between driving and driven pieces of rotating equipments. Although couplings can compensate for misaligned pieces of equipment, the need for accurate machinery rotating shaft alignments cannot be over emphasized. It is important to ensure proper machinery alignments allowing high cost capital equipments to last years instead of only months. In every industry there is a need to ensure proper machinery alignment since misalignment can cause damage amounting to many millions of dollars. Damage to equipments due to shaft misalignment is in the form of bearing failure due to excessive rub as well as destructive vibrations.

Misalignments of rotating machinery drive and driven elements occur as angular, lateral or as combinations of the two. Figure 6-4 depicts the various misalignment configurations. In parallel misalignment the two shafts are parallel but are not coaxially aligned (see figure 6-4(a)). Angular misalignments occur when the ends of the shafts to be coupled are laterally aligned but the shafts are not parallel. A configuration in which the driven shaft is angularly misaligned to the driving shaft is shown in figure 6-4(b). To further visualize angular misalignment,

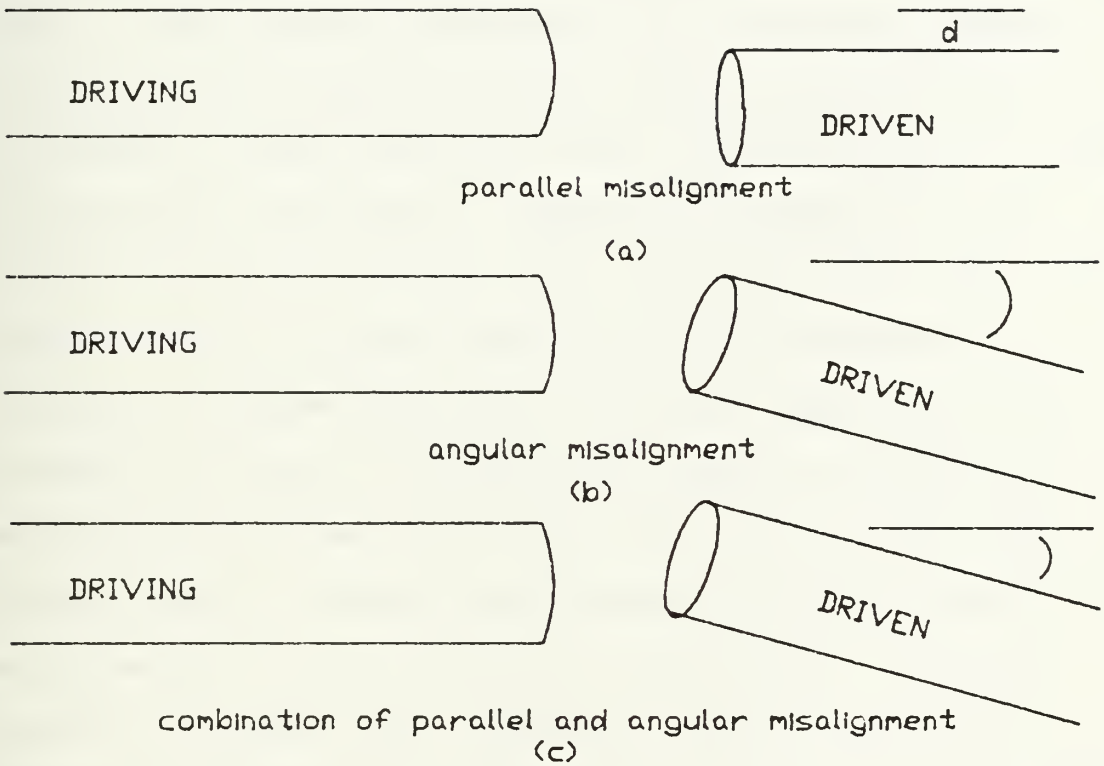

ALIGNMENT CONFIGURATIONS

FIGURE 6-4

if the shafts can be brought into alignment by moving one end of either or both shafts to correct the misalignment condition, the shafts can be said to exhibit purely angular misalignment. In figure 6-4(b) the shafts can be brought into alignment by raising the right hand end of the driven shaft. The amount or magnitude of misalignment present or tolerable in a coupled rotating system is usually specified as offset or total indicator runout (TIR). Offset is defined as the amount one shaft is physically displaced from its "truely" aligned position when measured from the other shaft. Total indicator runout is the difference in dial indicator readings taken in a particular plane when the dial indicator attached to one shaft is rotated 180 degrees. The relationship between offset and TIR can be expressed as offset = TIR/2. Methods for determining TIR and offset will be addressed in the following paragraphs. However, it should be noted that measured offset alone does not determine the type (i. e. angular, lateral or combinations of the two) of misalignment present. To clarify alignment criteria, alignment tolerances should be specified in amounts of angular and lateral misalignment allowable. In addition, the total amount of offset should be specified when combinations of lateral and angular misalignment are present.

Currently, the most common means of determining shaft element misalignments are dial indicator techniques and laser-optical alignment methods. Determining the amount of misalignment is usually done with dial indicator gages in configurations similar to those of figure 6-5. Indicator readings are taken in the following manner. With the dial indicators connected as shown the gages are initialized by adjusting the readings to zero at the respective shaft's twelve o'clock positions. Holding shaft B fixed, shaft A and its attached dial indicator is rotated slowly about its axis stopping at ninety degree intervals to record the indicator reading. (Readings should be recorded at the 3, 6, 9 and 12 o'clock positions for reasons to be discussed in following paragraphs.) The dial indicator should then be stopped at the 12 o'clock position to ensure the reading is still zero. It is a good idea to repeat the readings for verification. Then hold shaft A fixed and rotate shaft B and record the readings of indicator B in a similar manner. The recorded readings should look similar to figure 6-6. Adjustments to the rotating equipment foundations can only be accomplished by moves in either the horizontal, vertical or axial directions. This is why readings were recorded at only the 3, 6, 9 and 12 o'clock positions. When aligned the readings of gages A and B of figure 6-5 should be equal to zero throughout each shaft revolution. Again noting that the TIR is the gross difference in readings taken with dial

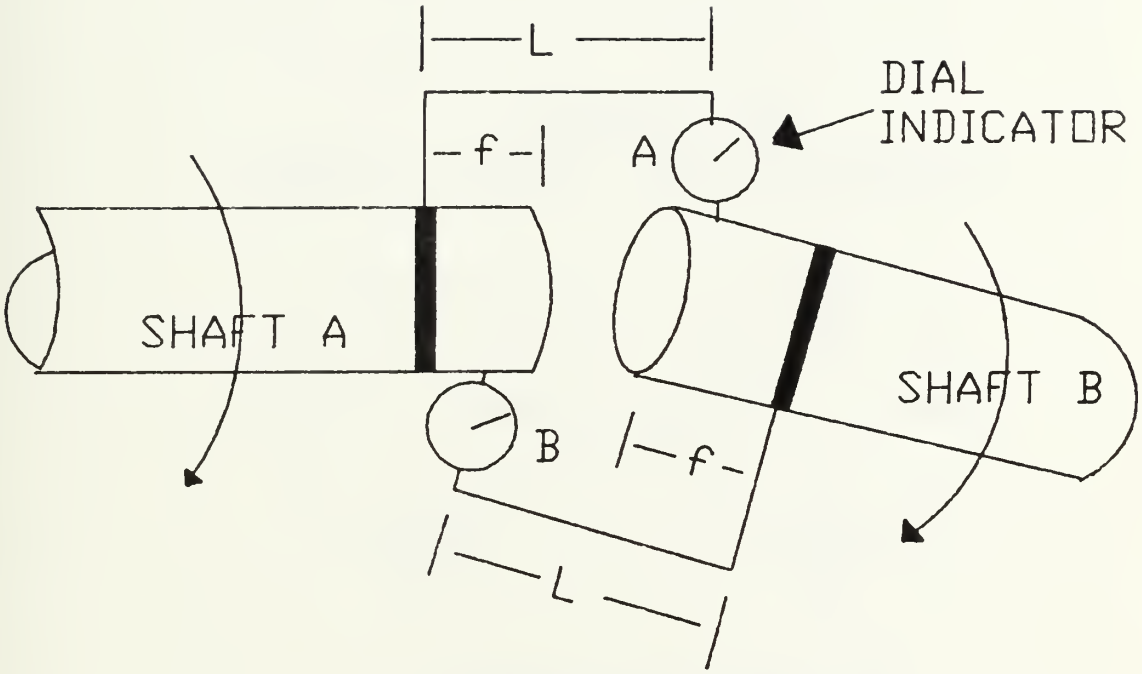

DIAL INDICATOR ARRANGEMENT

FIGURE 6-5

MEASURED FROM

DRIVER TO DRIVEN

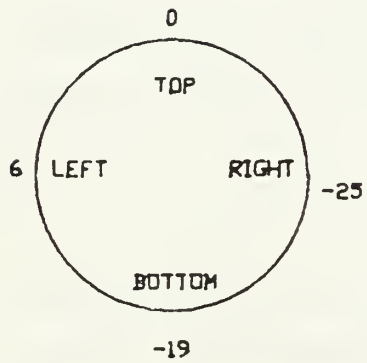

DRIVEN TO DRIVER

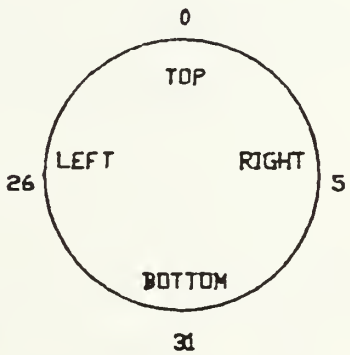

RECORDED DIAL INDICATOR
READINGS (IN MILS.)

FIGURE 6-6

indicators at the three and nine o'clock positions or twelve and six o'clock positions. Again, the amount of offset is TIR/2. It should also be clear that misalignment in the vertical plane will be indicated by the offset determined from the dial indicator readings taken in the twelve and six o'clock positions. Conversely, horizontal plane misalignment will be indicated by dial indicator readings taken in the three and nine o'clock positions. Misalignments are generally a combination of vertical and horizontal plane misalignments. However, for simplicity of explanation, the following paragraphs will assume the misalignment to occur in a single plane.

In general, misalignment conditions are usually combinations of parallel and angular misalignments. However, the cases of purely angular or purely parallel misalignments can be detected by dial indicator techniques. To determine if a misalignment is purely angular, determine the offset with the dial indicators in the horizontal or vertical planes as outlined above ensuring that the distances from the end of the shaft to the point where the dial indicator apparatus is fastened to the shafts are the same for each shaft. If the misalignment is purely angular the readings taken from the driver to driven shafts will correspond exactly to those readings taken from the driven to driving shafts for a particular plane. The angular offset component in the

horizontal or vertical planes is then determined by equation (1).

$$\text{Tan}(\theta) = (\text{indicator offset})/(L) \qquad (1)$$

where L is the distance between driving and driven shaft indicator connecting and measuring points. This distance should be the same for each dial indicator arrangement. The angle (θ) is the angle of misalignment.

To determine if a misalignment condition is a purely parallel misalignment, determine the offset with the dial indicators in either the horizontal or vertical planes by the same techniques expressed in the previous paragraphs. If the misalignment is purely parallel, the dial indicator readings taken from dial indicators A and B of figure 6-5 will be equal in magnitude but opposite in sign for a particular plane (either horizontal or vertical). The amount of misalignment is then expressed as:

$$\text{offset} = \text{TIR}/2 \qquad (2)$$

As noted above, misalignments generally occur as combinations of angular and parallel misalignments. In the cases of combined misalignment the dial indicator readings

taken from dial indicators A and B of figure 6-5 by the methods described above will differ in magnitude and sign. Using dial indicators to measure the misalignment offset when combinations of parallel and angular misalignment is present, will yield only the total offset. The amount of parallel or the degree of angular misalignment cannot be singularly isolated. For cases of combined misalignment, the misalignment is usually expressed simply as the TIR. In these cases the largest TIR from the two sets of readings (dial indicators A and B of figure 6-5) is regarded as the correct TIR. Consequently, to clearly express the allowable or existing coupling misalignment criteria, the alignment tolerances should be expressed in terms of amounts of angular misalignment (in degrees or radians), parallel misalignment (in mils or inches) and TIR (in mils or inches).

Currently, graphic methods for recording the indicator run-outs and determining the moves necessary to correct the misalignment are the most popular means of determining the alignment corrections. However, mathematical solutions exist which can be incorporated into hand held calculators and personal computers (Piotrowski, 1986).

The mathematical solution is obtained by making use of the fact that the shaft axes of the two rotating pieces of

equipment can be represented by straight lines corresponding to the axes center of rotation. Use of similar scalene triangles is then used to resolve the equipment moves. In figure 6-7 ht is the distance between points where the dial indicator is attached on one shaft and where it touches the other shaft. HT is the distance from where the indicator bracket is attached to the location of the inboard feet and HHT the distance to the outboard feet. The value bs is the shaft diameter on which the readings are taken. The BS and BBS terms are the magnitudes of the required moves of the inboard and outboard feet respectively. Similar triangle relationships can be obtained for each of the two pieces of equipment to be aligned. Consequently, correcting moves can be algebraically determined. The similar triangle relationships are then given by equation (3).

$$ht/bs = HT/BS = HHT/BBS \tag{3}$$

For the driven and driving elements shown in figure 6-7 required moves to bring the system into alignment in single plane can be calculated. Correcting moves for the driven and driving feet are calculated as follows.

Driver inboard feet:

$$IB_{DR} = B[\ X + Y\ ]/C - Y \tag{4}$$

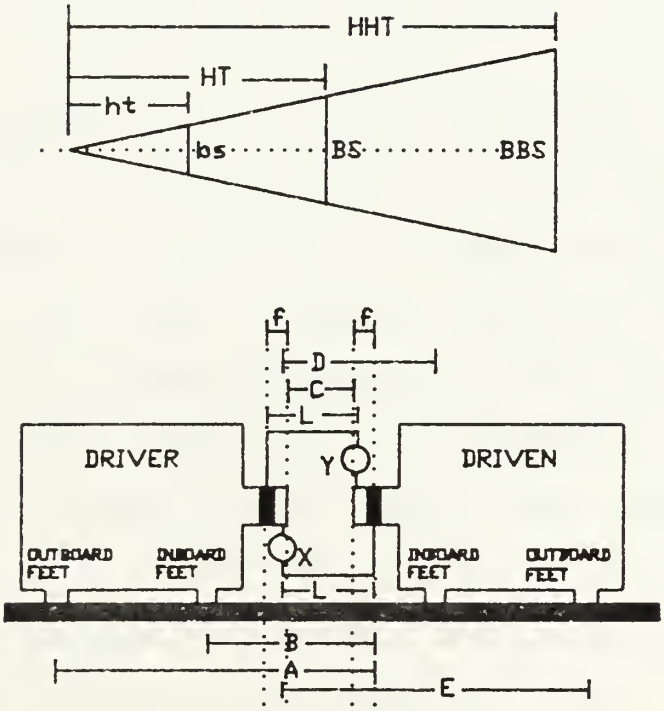

DIAL INDICATOR GEOMETRIES FOR MATHEMATICAL CALCULATIONS OF EQUIPMENT ALIGNMENT MOVES.

FIGURE 6-7

Driver outboard feet:

$$OB_{DR} = A[\ X + Y\ ]/C - Y \quad (5)$$

Driven inboard feet:

$$IB_{DN} = D[\ X + Y\ ]/C - X \quad (6)$$

Driven outboard feet:

$$OB_{DN} = E[\ X + Y\ ]/C - X \quad (7)$$

where:

X = one half the dial indicator readings taken with the dial indicator attached to the driven shaft and readings taken on the driving shaft.

Y = one half the dial indicator readings taken with the dial indicator attached to the driving shaft and readings taken on the driven shaft.

The other dimensions are shown on figure 6-7.

To complete the machinery alignment these calculations must be accomplished for moves in the vertical plane and again for the horizontal plane. Therefore, to accomplish alignment in one move of the equipment feet eight calculations must be performed. For horizontal moves, the indicator run-outs recorded in the three and nine o'clock positions are used. The vertical moves are determined using readings recorded in the twelve and six o'clock positions. In both cases positive values indicate that the equipment feet need to be raised or moved left. Negative values indicate the equipment feet must be moved right or down.

Although currently not as commonplace as dial indicator methods, the use of lasers to optically align shafts is becoming more popular. With the cost, size and ruggedness of these systems improving the laser system is becoming a more viable alignment tool for the twentieth century mechanic and technician. A laser-optical alignment system consists of a laser/detector unit and reflecting prism attached to the driving and driven shafts, a keyboard for data entry, micro processor with a display unit and connecting cables. In simple terms, the operation of the laser alignment system is as follows. The laser/detector unit is mounted on either the driving or driven shaft and trained toward the reflecting prism which is mounted on the other shaft. The prism reflects the laser beam back to the detector. In an initial position the reflected laser beam is zeroed onto the detector to establish a reference. The shaft is then rotated. As the reflected beam moves relative to the zeroed position during the rotation; the detector, micro processor and display units measure, calculate and display the amount the reflected beam deviates from the zeroed position. This operating principle can be seen in figure 6-8 (Piotrowski, 1986). By utilizing the keyboard, the correct geometric numerics for the equipment installation can be entered into the micro processor. Using entered data for the machinery installation and the measured deviations of the reflected beam, the alignment condition is

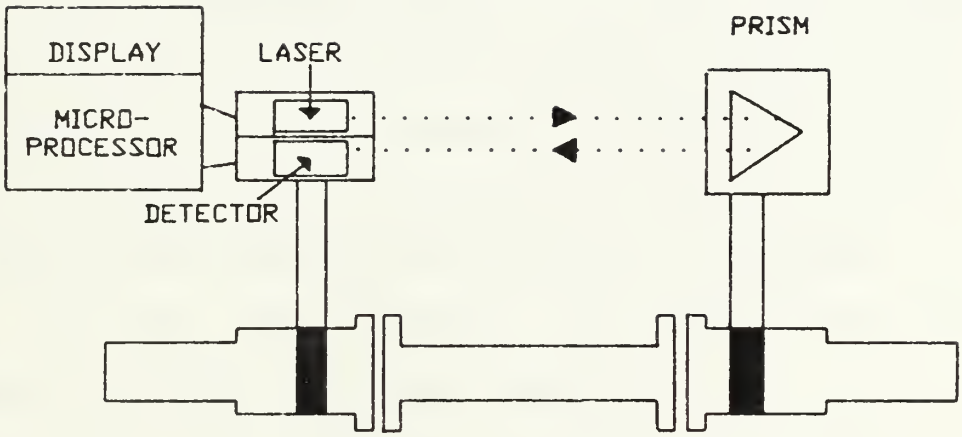

LASER OPTICAL ALIGNEMT SYSTEM

FIGURE 6-8

visualized on the display unit together with the necessary moves to bring the system into alignment.

The advantages of the laser optical system over dial indicator methods are many. Set up time is much faster; in fact Bloch (1987) reported that in a Canadian power generation plant, alignments which normally took eleven days with dial indicator methods took only five days with laser alignment techniques. Laser optical readings can be taken with the coupling in place or removed. This allows a check to be done with out a need to uncouple the rotating devices. Distance between driving and driven pieces of equipment is no longer critical. The accuracy and repeatability of measurements are vastly improved. Lastly, visual representation of the misaligned condition and required moves are automatically calculated and displayed. Disadvantages of the laser optical systems are cost of equipment and relative fragileness of the components.

In preceding sections of this report the results of equipment misalignments have been discussed. The issue of how much a system can deviate from the "perfectly" aligned position has not been generally agreed upon by machinery manufacturers. Figure 6-9 shows a variety of guide lines established by several organizations and individuals. In general it is agreed that alignment tolerances are angular

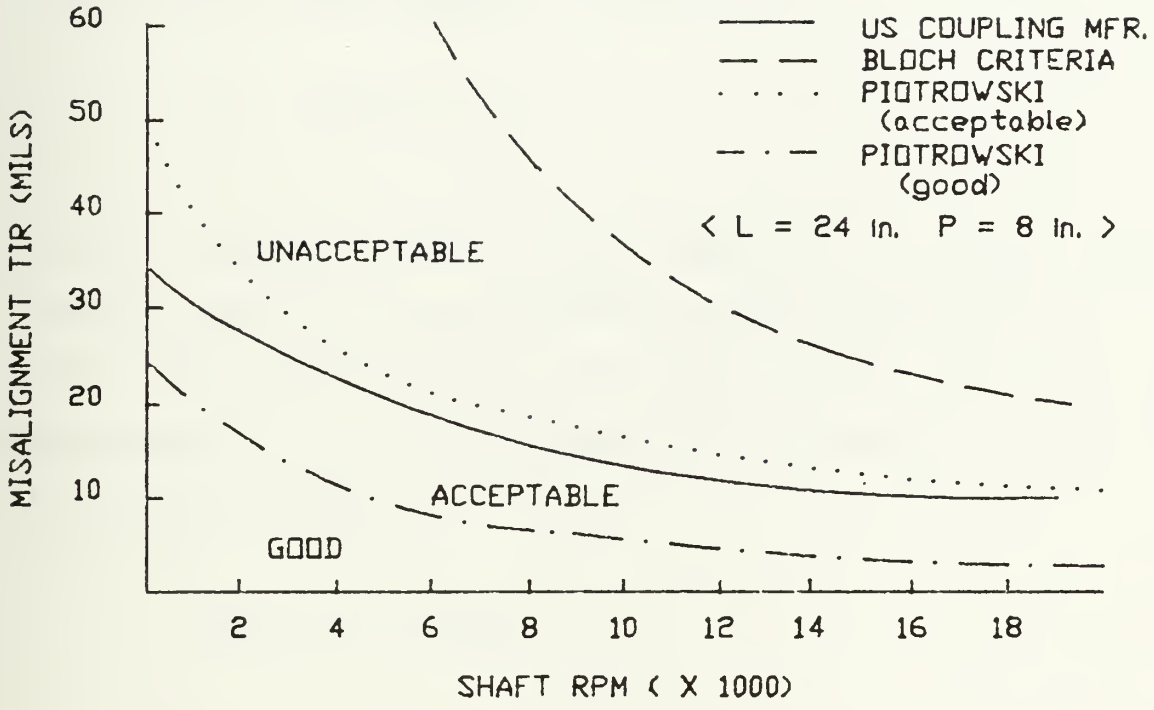
MISALIGNMENT TIR (MILS)
60
50
40
30
20
10
UNACCEPTABLE
ACCEPTABLE
GOOD
2
4
6
8
10
12
14
16
18
SHAFT RPM (X 1000)
US COUPLING MFR.
BLOCH CRITERIA
PIOTROWSKI (acceptable)
PIOTROWSKI (good)
< L = 24 in. P = 8 in. >

FIGURE 6-9

velocity dependent. This stems from two criteria. When a misalignment causes system unbalance, the vibrational amplitude increases in proportion to the rotational frequency squared. Secondly, for gear couplings to maintain proper lubrication the sliding velocity of the engaged teeth should not exceed 120 inches per minute (Bloch, 1987). Equation (8) approximates this velocity.

$$V = DN(\tan(\theta)), \tag{8}$$

where D equals the gear pitch diameter, N is the shaft angular velocity in revolutions per minute and 2[tan(θ)] is the total indicator run-out divided by the coupling hub separation (L). An expression for the amount of allowable offset would then be:

$$TIR/L = V/(DN). \tag{9}$$

Equation (9) shows the allowable TIR to be a function of one over the angular velocity. This relationship is shown on figure 6-9. A second curve on figure 6-9 shows a recommendation of a US coupling manufacturer for gear couplings (Bloch, 1987). This curve utilizes equation (10) to determine allowable offsets.

$$TIR = [\, L/P + 1]M. \tag{10}$$

In equation ten (L) is the length between coupling gear teeth centers, P is the gear tooth pitch diameter and M is a velocity dependent coefficient. The third set of tolerance criteria shown in figure 6-9 were published by Piotrowski; (1986). In this figure Piotrowski's allowable offset per inch of shaft separation was converted to a measure of TIR for L equal to 24 inches and P equal to eight inches. The figure also shows a relative measure of alignment tolerance merit. Depending on the type of coupling, the velocity of the drive and the application, operation in any of the ranges may be "acceptable". For diaphragm couplings very little misalignment is allowable due to fatigue considerations, so operation in the "good" region is desirable. For universal joints and gear couplings operation in the acceptable region of figure 6-9 may be adequate. In general the velocity dependence tends to be derived from the gear coupling requirements. However for other types of couplings, bearing rub, fatigue failure and unbalanced vibrational amplitude are also velocity dependent and must be considered. For constant velocity couplings which do not exhibit vibrational misbehavior or unbalance due to misalignment, the coupling alignment criteria is not velocity dependent. In the case of constant velocity couplings the allowable total indicator run-out is governed by the mechanical limitations of the particular coupling geometry. The discussion in section 3.3 of this study

outlines the configurations in which constant velocity couplings can be used to compensate for considerable amounts of angular and/or lateral misalignment. For these applications the degree of allowable misalignment is not angular velocity dependent but rather dependent on the mechanical construction of the flexible couplings. Criteria for these couplings would plot as horizontal lines on figure 6-9 corresponding to the TIR of the particular coupling specification.

In conclusion, allowable alignment tolerances depend on the type of coupling and the application. No general agreement has been reached on how much misalignment is acceptable. However, there is agreement that the amount of allowable misalignment decreases inversely to the driving angular velocity.

7.0 COUPLINGS

To ensure that the rotor of a piece of rotating machinery is sufficiently designed to withstand the stresses and strains of the operating environment, the coupling chosen to join the driving and driven mechanisms must be properly selected. In addition to transmitting torque from the driving to the driven pieces of machinery, the coupling must also compensate for intentional and/or unintentional misalignments and allow for possible axial motion of the rotating devices. Rotating drivers involve equipments with horsepower ratings of less then a single horsepower to turbines rated at 60,000 horsepower or more rotating at angular velocities of a few revolutions per minute to 100,000 revolutions per minute (Piotrowski, 1986). The proper choice of couplings used to connect these drivers to their corresponding components is a critical issue. Proper selection depends upon the characteristics of the driving and driven work-pieces, the operating environment and operating life expectancies of the machinery. The coupling must be capable of operating at the maximum designed horsepower and speeds of the machinery. In most cases the coupling is not chosen to be the weak link in that failure of the coupling in some instances would cause severe damage

to either the driving or driven or both pieces of machinery. The misalignment capacity of the coupling must be sufficient to account for installation offsets, misalignment due to thermal expansion or contractions and dynamic misalignments encountered when equipments are located on moving platforms. Often the coupling must be able to absorb large axial thrust due to loading or unloading of the driven equipments as in propulsion turbines and engines. The torsional stiffness of the coupling must be compatible with both the driving and driven components. In some installations a coupling that will dampen large torsional fluctuations may be desirable while in other instances the coupling application will call for torsional rigidity. The coupling's expected service operating temperature range must be known. This aides in proper material selections. Material characteristics are often temperature dependent in that in cold temperature the coupling components may become brittle while at high temperatures a loss of strength may be observed. Lastly, the driving and driven shafts mechanical connecting geometries and material characteristics must be known. The connecting mechanism on the coupling must mate in size and geometry to the shafts. In addition, the thermal characteristics of the connecting shafts must be specified so that expansion or contraction of the shafts and coupling will not weaken the mechanical joint. As alluded to in previous sections of this paper there is a large variety of

coupling types. Six major categories of couplings will be briefly outlined below. The rigid couplings discussed in section 3.1 consist of a variety of devices which directly fasten the driving to the driven equipments with no capacity for compensating for axial, lateral or angular misalignments. Gear couplings are used to join pieces of equipment primarily when speed increases or decreases are desired. These couplings involve mating of the machinery components through various teeth or chain-teeth contacts with speed variations accomplished by the driving to driven gear diameter ratios. Slight misalignments are accounted for in either loose fitting or sliding of mating parts. Grid couplings are couplings in which hubs are placed on the connecting ends of the rotating elements. These hubs must be the same diameter and slotted such that slots of the driver mate exactly with the slots of the driven hub (see figure 7-1). A metallic grid is then placed in the slots in an inter-woven fashion. These couplings can accommodate axial, angular and lateral misalignments due to the flexibility of the grid. In addition, this coupling allows for torsional flexibility when changing loads, shock or vibrations are imposed on the system. Grid couplings yield vibration data corresponding to even multiples of the drive shaft angular velocity when misaligned. These vibrational characteristics are due to the flexing of the metalic grid two times per drive shaft revolution when misaligned

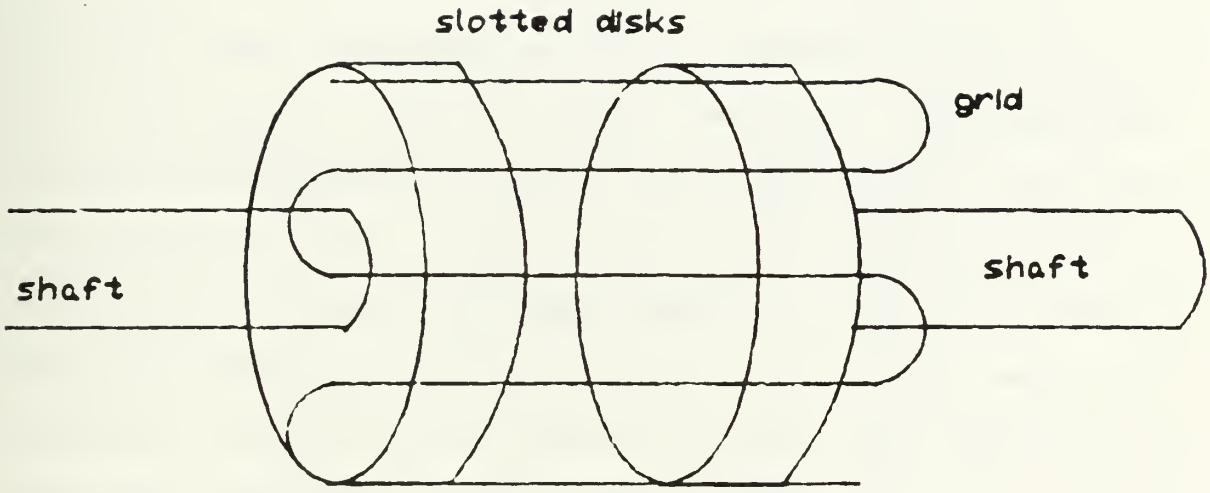

Grid coupling

FIGURE 7-1

(Piotrowski, 1986). The fourth and fifth major categories of couplings are the universal or Cardan joints and rubber couplings which have been discussed in sections 3.2, 3.3 and 4.0 of this paper. The final category of couplings are disk couplings. These couplings consist of multiple flexible disks which are alternately fastened to each other and the driving and driven shafts (see figure 7-2). These couplings can accommodate varying degrees of axial, angular and lateral misalignments as well as torsional load variations.

As can be seen, the selection of the proper coupling for a given application can be quite complex. The selection process is further complicated in that the various coupling manufactures do not always provide the design criteria sought when incorporating the coupling into the design. Certainly, there is a minimum set of requirements needed to ensure at least a minimal degree of success when selecting a coupling. The four basic requirements are the maximum horsepower rating, highest operating angular velocity, allowable alignment tolerances and the mechanical coupling size and geometry needed to fasten the coupling to the shafts. In addition input versus output speed variations would be useful, especially in applications where constant angular velocity outputs are desired.

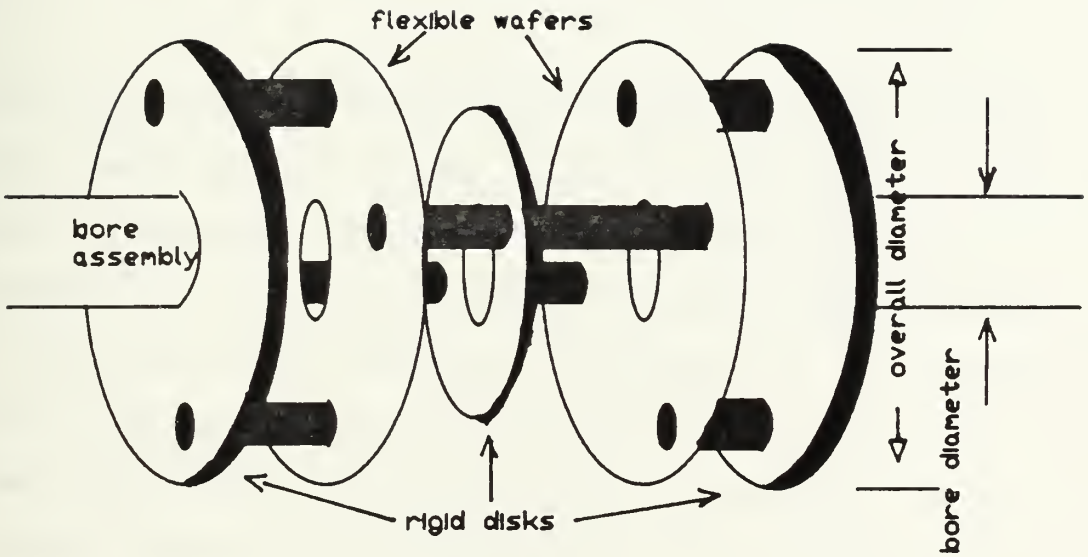

Disk type flexible coupling

FIGURE 7-2

7.1 Disk Coupling Analysis

To illustrate the complexities of coupling selection an "off the shelf coupling" will be analyzed. The discussion will include angular velocity, horsepower ratings, alignment criteria, coupling size and geometries, dynamic characteristics and possible failure modes. The coupling selected for this study is a flexible disk coupling manufactured by Renbrandt, Inc. of Boston Massachusetts. The specifications supplied with the coupling are shown in table 7-1.

The first item of business is to determine which column of the specifications apply to the particular coupling. Physical measuring of the device determines that the overall diameter is 1.5 inches indicating column three is applicable to this particular coupling. See figure 7-2 for a sketch of this coupling. The torque rating is 250 in.-oz. and maximum RPM is 5000 which indicates that the maximum torque and angular velocity to be delivered by the driver must be less than these values. The alignment criteria for this coupling is specified in both angular, parallel and total allowable misalignment. The degree of existing misalignment can be determined by methods described in section 6.2 of this study.

Renbrandt Flex-mite couplings are not designed for applications in excess of the following ratings:

SERIES	1	2	3
Overall diameter	.75 in.	1.0 in.	1.5 in.
Bore sizes (inches)	1/16 - 1/4	1/16 - 3/8	1/16 - 5/8
Static torque rating	30 in-oz	60 in-oz	250 in-oz
Max. angular misalignment	3 deg.	3 deg.	3 deg.
Max. parallel misalignment	.010 (in)	.015 (in)	.018 (in)
Total indicator misalignment (inches)	.020 T.I.R.	.030 T.I.R.	.035 T.I.R.
RPM	5000	5000	5000

Renbrandt flexible coupling No. B55C55c specification sheet.

Table 7-1

The flexibility of a disk type flexible coupling is accomplished by the thin flexible wafers shown in figure 7-2. The coupling bore assemblies and center disk are rigid and are not designed to flex during rotation of the coupling. When the disk coupling is used to connect two pieces of equipment that are misaligned the flexible wafers continually bend as the coupled shafts rotate. Consequently, both angular and parallel misalignments are compensated for by bending action of the dual flexible wafers. This bending action gives rise to fatigue during operation in misaligned configurations which is the primary cause of failure for metallic disk couplings. Obviously, the greater the degree of misalignment the shorter the coupling life with other parameters held constant. To analyze the output angular velocity characteristics, the basic requirements for a constant velocity couplings should be re-stated.

(1) The driving and driven shafts plane of contact must be constant in space throughout each revolution.
(2) The plane of contact point rotation must remain normal to the plane defined by the rotating shafts.
(3) This plane of contact must exactly bisect the angle made by the offset shafts.
(4) The shafts must lie in the same plane.

For the disk coupling depicted in figure 7-2 the driving and

driven plane of contact is defined by the center disk. As the shafts rotate in a misaligned condition the flexible disks deflect equally allowing the center disk plane of rotation to remain fixed throughout each shaft revolution. This center disk also remains normal to the plane defined by the driving and driven shafts. The flexible disk coupling is analogous to a double universal joint coupling. Each of the two flexible disks correspond to the universal joints and the center rigid disk corresponds to the coupling shaft. Due to action and reaction forces imposed on the flexible disks by the misaligned shafts, the rigid center disk will be pushed and pulled into a position of equilibrium such that the obtuse angle formed by the two shafts will be exactly bisected. Thus the conditions required for constant velocity couplings are achieved. A critical issue for this type of coupling is the material of the flexible disks. These disks must resist surface fatigue while maintaining constant flexibility parameters throughout its life. In addition the disks must exhibit identical properties. If the elasticity of the flexible disks are different the equilibrium position of the center disk will not bisect the obtuse angle formed by the shafts and constant velocity characteristics will be lost.

7.2 Disk Coupling Failure Analysis

To assess the fatigue resistance of the coupling, a dynamic analysis of the coupling's flexible disks must be performed. For this analysis take the case of the maximum angular misalignment (i.e. 3 degrees) at the maximum angular velocity (5000 rpm). This alignment scheme can be seen in figure 7-3. As the coupling rotates, the point where the coupling bore assemblies attach to the flexible disks will be alternately displaced by one-half the total angular misalignment. In addition, an out of plane twist will be imposed on the wafer equal to one-half the angular misalignment. These cyclic displacements could give rise to fatigue failure if the stress placed on the coupling flexible disks is greater than the flexible disks "endurance limit". The endurance limit of a material is defined as the stress in which regardless of the number of loading cycles fatigue failure does not occur. The endurance limit for steels in bending is generally twice the endurance limit of the same specimen in torsion. Therefore, a good design criteria for the endurance limit of a material undergoing both bending and torsion (i.e. combined stresses) is approximately fifty percent of the endurance limit for bending stresses (Timoshenko, 1930).

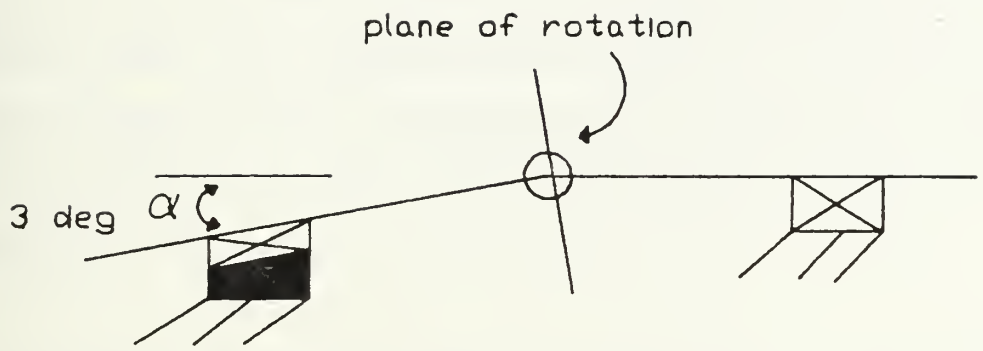

Flexible disk coupling with angular misalignment

FIGURE 7-3

It should be noted that endurance limits of materials are determined experimentally. Endurance limits are functions of the types of applied stresses, the directionality of the applied stresses, the material properties, and sample geometries. While the endurance limit of all materials cannot be expressed in terms of the material properties, for steels sufficient data exists to support a correlation for the endurance limit in bending to be approximately equal to fifty percent of the ultimate tensile strength of the material.

In selecting a coupling, the fatigue life of the coupling should ideally exceed the life of the equipment or at least exceed the time between planned overhauls. To determine if the coupling's flexible wafers are susceptible to fatigue the magnitude of the combined applied stresses need to be determined. The compounding effects of the combined action of bending and twisting is represented by equation (3) (Timoshenko, 1930).

$$\tau_c = ((\sigma_x/2)^2 + (\tau_t)^2)^{1/2} \qquad (3)$$

In equation (3) τ_c is the cumulative stress on the flexible disk due to both bending and twisting at any point on the disk. The stress due to bending is σ_x and the stress due to twisting is τ_t.

When the coupling is angularly misaligned as in figure 7-4, the deflection of the flexible wafer can be represented by equation (4).

$$d = R\sin(\alpha/2) \qquad (4)$$

Consequently, for a misalignment angle of three degrees the total out of plane deflection is .014 inches, and the maximum angular twist placed on the cross section is 1.5 degrees.

In his analysis of "Bending of a Curved Bar Out of its Plane of Initial Curvature", Timoshenko (1930) utilized Castigliano's theorems and the principle of least work to determine the deflection of a curved beam due to combined bending and twisting. For an imposed force (P) and moment (M_{xt}), the potential energy for these combined actions for the curved beam of figure 7-5 can be written as:

$$V = \int_0^{\alpha} [(M_x/(2EI_x))^2 + (M_y/(2EI_y))^2 + (M_z/(2C))^2]Rd\varphi. \qquad (5)$$

In equation (5) M_x and M_y are the moments on the cross section due to bending and M_z is the moment on the beam cross section brought on by the twisting action due to load P and moment M_{xt}. For a load placed on the beam in the "y" direction the M_y term is zero,

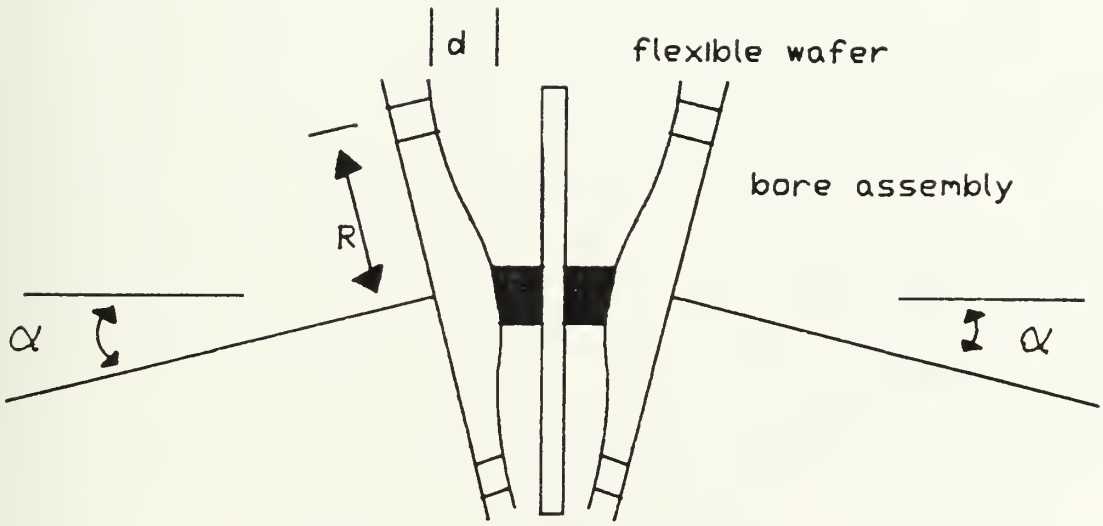

Misaligned disk coupling

FIGURE 7-4

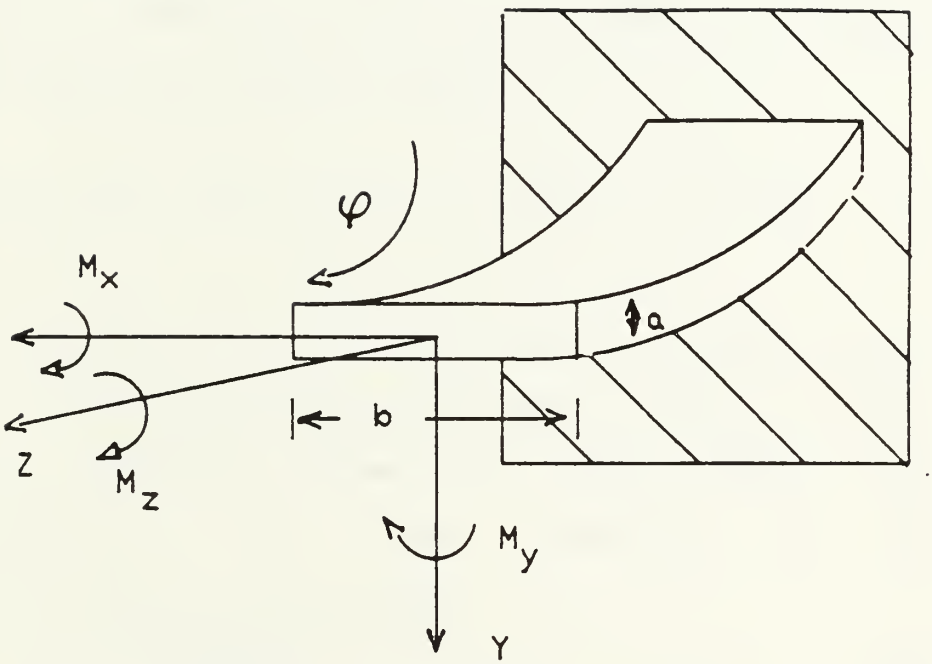

Cross section of curved clamped beam

FIGURE 7-5

$$M_x = -PR\sin(\alpha - \varphi) \qquad (6)$$

and

$$M_{zp} = PR(1 - \cos(\alpha - \varphi)). \qquad (7)$$

Applying Castigliano's second theorem yields:

$$(dV/dP) = d. \qquad (8)$$

Combining equations 5, 6, 7, and 8 yields the following expression for the deflection of a curved beam in bending and torsion due to the applied load P.

$$d = \int_0^{\alpha} PR[(\sin^2(\alpha - \varphi))/EI_x + (1 - \cos(\alpha - \varphi))^2/C]d\varphi. \qquad (9)$$

For the semi-circular beam of figure 7-6 the central angle is equal to π, the location of the load is equal to $\pi/2$. I_x is the x - component moment of inertia and C the torsional rigidity of the beam. Carrying out the integration of equation (9) yields:

$$d = P(.655). \qquad (10)$$

For the case of three degrees of angular misalignment d is .014 inches. Inserting this value into equation (8) yields the load required to accomplish the deflection.

$$P = .022 \text{ lbs.} \qquad (11)$$

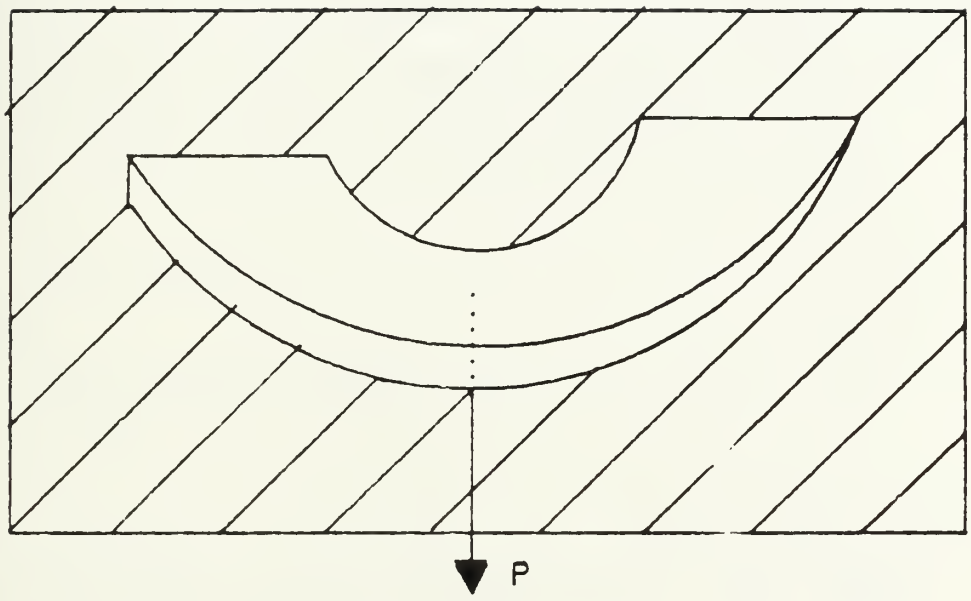

SEMI-CIRCULAR CURVED BEAM LOADED AT THE CENTER

FIGURE 7-6

The total angular twist imposed on the flexible wafer by the shafts angular misalignment has two components; the component due to the imposed load and the component due to the applied moment M_{zt}. The maximum angular twist on the beam is .026 radians which occurs at the point of the applied load and moment. Assuming linearity, the angle of twist per unit length around the circumference equates to .03 radians per inch. Therefore, the twist per unit length due to the load (P) can be expressed as:

$$\theta_p = M_{zp}/C \qquad (12)$$

where

$$M_{zp} = PR(1 - \cos(\alpha - \varphi)). \qquad (13)$$

Solving equation (12) yields θ_p = .0148 radians per inch. Thus the twist per unit length due to the applied moment (M_{zt}) can be expressed as:

$$\theta_t = \theta_{max} - \theta_p \qquad (14)$$

where θ_{max} is the maximum twist per unit length. Utilizing equation (14) determines: θ_t = .0153 radians per inch. Solving for the applied twisting moments:

$$M_{zt} = \theta_t/GC \qquad (15)$$

yields:

$$M_{zt} = .01255(1 - \cos(\alpha - \varphi)).$$

Using the principles of superposition the sum of the twisting moments is:

$$M_z = M_{zp} + M_{zt} \qquad (16)$$

which yields:

$$M_z = .03(1 - \cos(\alpha - \varphi)). \qquad (17)$$

The stresses at any particular cross section can be written as:

$$\sigma = M_x c / I, \qquad (18)$$

$$\tau = M_z / C_o \qquad (19)$$

where c is the distance to the neutral axis; and C_o, the polar moment of inertia, is equal to $1/3ba^2$ for a thin beam. Solving for the maximum stress due to the bending and torsion combination (which occurs at the endpoints) yields:

$$\sigma_{xmax} = 2836 \text{ psi}$$

$$\tau_{tmax} = 3519 \text{ psi}$$

Inserting these values into equation (3) yields the maximum stress due to the combined bending and twisting.

$$\tau_{cmax} = 3793 \text{ psi}$$

A typical value for the endurance limit of stainless steel is 25,000 psi. The cyclic stress placed on the coupling's flexible disk is therefore significantly less than the design endurance limit. Consequently, for the maximum angle of misalignment fatigue failure of the Renbrandt coupling should not occur.

At this point it should be readily apparent that the selection of a coupling for a particular application is a complex issue. The degree of difficulty depends on the application requirements. In high power high speed applications coupling issues become paramount in maintaining service and service life as well as protecting costly pieces of equipment.

LIST OF REFERENCES:

Bloch, Heinz P., 1987, "Making Ends Meet - Laser-Optic Alignment of Shafts", Mechanical Engineering, November, 1987, pp. 56 - 63.

Bucciarelli, L. L., 1982, "On the Instability of Rotating Shafts Due to Internal Damping", Journal of Applied Mechanics, June 1982, Vol. 49, pp. 425 - 428.

Costa, A., 1982, "Inconsistant - Velocity Drives Incorporating Two Cardan Joints: The Present State of Knowledge and Design of Experimental Research", Meccanica, Vol. 17, pp. 179 - 200.

Costa, A. and Davoli, P., 1983, "An Experimental Investigation on Torsional Oscillations in Constant Velocity Two-Cardan Joint Drives", Meccanica, Vol. 18, pp. 34 - 53.

Crandall, S. H., 1980, "Physical Explanation of Destabilizing Effects of Damping in Rotating Parts", Rotardynamic Instability Problems in High Performance Turbomachinery, NASA, CP. 2133, pp 1 - 18.

Crandall, S. H., 1983, "The Physical Nature of Rotor Instability Mechanisms", Rotor Dynamic Instability, M. L. Adams, editor, AMD. - Vol. 55, ASME, NY.

Den Hartog, J. P., 1956, Mechanical Vibrations, McGraw-Hill Book Company, New York, pp. 429 - 433.

Dimentberg, F. M., 1961, Flexural Vibrations of Rotating Shafts, Translated by: Production Engineering Research Association, Butterworths.

Harris, C. M., ed., 1961, Shock and Vibration Handbook, Vol. 1, McGraw-Hill Book Company, New York, pp. 1-1 - 1-13.

Iwatsubo, T. and Saigo, M., 1984, "Transverse Vibration of a Rotor System Driven by a Cardan Joint", Journal of Sound and Vibration, Vol. 95, pp. 9 - 18.

Mancuso, Jon R., 1986, Couplings and Joints, Marcel Dekker, Inc., New York and Basel, pp. 415 - 418.

Masabuchi, Koichi, 1980, Analysis of Welded Structures, Pergamon Press, New York, pp. 450 - 614.

Maxwell, J. H., 1980, "Vibration Analysis Pinpoints Coupling Problems", Hydrocarbon Processing, Jan. pp. 95 - 98.

Nichols, J. C., 1976, "Effect of Residual Shaft Bow on Unbalance Response and Balancing of a Single Mass Flexible Rotor", Engineering for Power, Vol. 98, No. 2, pp. 82 - 107.

Norris, C. H., Wibur, J. B. and Utka, S., 1960, Elementary Structural Analysis, McGraw-Hill Inc., New York, pp. 213 - 278.

Ota, H. and Kato, M., 1984(a), "Lateral Vibrations of a Rotating Shaft Driven by a Universal Joint", Bulletin of JSME, Vol. 27, No. 231, pp. 2002 - 2007.

Ota, H. and Kato, M., 1984(b), "Unstable and Forced Vibrations of an Asymmetrical Shaft Driven by a Universal Joint", Vibrations in Rotating Machinery, York, UK, I. Mech. E., pp. 493 - 498.

Ota, H. and Kato, M. and Hiroshi, S., 1985, "Lateral Vibrations of a Rotating Shaft Driven by a Universal Joint - second report", Bulletin of JSME, Vol. 28, No. 242, pp. 1749 - 1755.

Piotrowski, John, 1986, Shaft Alignment Handbook, Marcel Dekker, Inc., New York and Basel, pp. 1 - 8, 108 - 114 and 231 - 234.

Porat, I., 1980, "Moment Transmission by a Universal Joint", Mechanisms and Machine Theory, Vol. 15, pp. 245 - 254.

Timoshenko, S., 1930, Strength of Materials, part II, D. Van Norstrand Company, Inc., pp. 467 - 473.

Timoshenko, S., 1960, Elements of Strength of Materials, D. Van Norstrand Company, Inc., pp. 183 - 257.

Wiederrich, J. L., 1982, "Analysis of Drive Shaft Speed Variations in a Scotch Yoke Mechanism", Journal of Mechanical Design, Vol. 104, pp. 239 - 246.

Yanabe, S. and Fuwano, M., 1985, "Rotor Axial Vibration Caused by Gear Couplings", Bulletin of JSME, Vol. 28, No. 241, pp. 1497 - 1506.

Thesis
B21695 Barber
c.1 Vibration problems of
rotating machinery due to
coupling misalignments.